Time-dependent properties of run-and-tumble particles. II. Current fluctuations

Tanmoy Chakraborty [*] and Punyabrata Pradhan [†]

*Department of Physics of Complex Systems, S. N. Bose National Centre for Basic Sciences, Block-JD,
Sector-III, Salt Lake, Kolkata 700106, India*

We investigate steady-state current fluctuations in two models of hardcore run-and-tumble particles (RTPs) on a periodic one-dimensional lattice of L sites, for arbitrary tumbling rate $\gamma = \tau_p^{-1}$ and density ρ; model I consists of standard hardcore RTPs, while model II is an analytically tractable variant of model I, called a long-ranged lattice gas (LLG). We show that, in the limit of L large, the fluctuation of cumulative current $Q_i(T, L)$ across the ith bond in a time interval $T \gg 1/D$ grows first subdiffusively and then diffusively (linearly) with T: $\langle Q_i^2 \rangle \sim T^\alpha$ with $\alpha = 1/2$ for $1/D \ll T \ll L^2/D$ and $\alpha = 1$ for $T \gg L^2/D$, where $D(\rho, \gamma)$ is the collective- or bulk-diffusion coefficient; at small times $T \ll 1/D$, exponent α depends on the details. Remarkably, regardless of the model details, the scaled bond-current fluctuations $D\langle Q_i^2(T, L) \rangle / 2\chi L \equiv \mathcal{W}(y)$ as a function of scaled variable $y = DT/L^2$ collapse onto a universal scaling curve $\mathcal{W}(y)$, where $\chi(\rho, \gamma)$ is the collective particle mobility. In the limit of small density and tumbling rate, $\rho, \gamma \to 0$, with $\psi = \rho/\gamma$ fixed, there exists a scaling law: The scaled mobility $\gamma^a \chi(\rho, \gamma)/\chi^{(0)} \equiv \mathcal{H}(\psi)$ as a function of ψ collapses onto a scaling curve $\mathcal{H}(\psi)$, where $a = 1$ and 2 in models I and II, respectively, and $\chi^{(0)}$ is the mobility in the limiting case of a symmetric simple exclusion process; notably, the scaling function $\mathcal{H}(\psi)$ is model dependent. For model II (LLG), we calculate exactly, within a truncation scheme, both the scaling functions, $\mathcal{W}(y)$ and $\mathcal{H}(\psi)$. We also calculate spatial correlation functions for the current and compare our theory with simulation results of model I; for both models, the correlation functions decay exponentially, with correlation length $\xi \sim \tau_p^{1/2}$ diverging with persistence time $\tau_p \gg 1$. Overall, our theory is in excellent agreement with simulations and complements the prior findings [T. Chakraborty and P. Pradhan, Phys. Rev. E **109**, 024124 (2024)].

I. INTRODUCTION

Characterizing the time-dependent properties of interacting self-propelled particles (SPPs), also known as active matter, has attracted a lot of attention in the past [1,2]. SPPs convert chemical energy into directed or persistent motion ("run"); they move with a velocity v and randomly change directions, or tumble, with a rate γ, thus violating detailed balance (i.e., breaking time-reversal symmetry) at microscopic scales and driving the system out of equilibrium. Because of the delicate interplay between persistence and interactions, they display remarkable collective behavior, such as flocking [3], clustering [4], "giant" number fluctuation [5], and anomalous transport [6,7]. Indeed, over the last couple of decades, significant effort has been made to better understand the emergent properties of active matter through studies of paradigmatic models, such as the celebrated Vicsek models [3], active Brownian particles (ABPs) [8] and run-and-tumble particles (RTPs) [9]. However, despite numerous simulation and analytical studies in the past [1,2], theoretical characterization of the dynamic properties of these many-body systems poses a major challenge and is still far from complete.

There is a well-established statistical mechanics framework for many-particle systems satisfying detailed balance.

For example, consider a one-dimensional "diffusive" system in a near-equilibrium scenario; the time evolution of coarse-grained local density $\rho(x, \tau)$ at suitably rescaled space x and time τ can be described by a fluctuating hydrodynamic equation,

$$\frac{\partial \rho(x, \tau)}{\partial \tau} = \frac{\partial}{\partial x}\left[D(\rho)\frac{\partial \rho}{\partial x} + \sqrt{\frac{2\chi(\rho)}{L}}\zeta_x(\tau) \right], \quad (1)$$

which is written in terms of two density-dependent transport coefficients—the collective- or bulk-diffusion coefficient $D(\rho)$ and the mobility $\chi(\rho)$; here $\zeta_x(\tau)$ is the Gaussian white noise with unit variance and L is the system size. Perhaps not surprisingly, for systems violating detailed balance (nonequilibrium), there is no general theoretical framework. However, in recent times, a deeper understanding of the problem for a broad class of diffusive, albeit nonequilibrium, systems is gradually emerging through the formulation of macroscopic fluctuation theory (MFT) [10]. Quite remarkably, MFT proposes a similar description as given in Eq. (1), even when detailed balance is violated in the bulk of the system. Of course, calculating the macroscopic transport coefficients $D(\rho)$ and $\chi(\rho)$ for interacting systems is a nontrivial task, especially when the system is driven out of equilibrium and its nonequilibrium steady-state measure is *a priori* not known. Notably, the bulk-diffusion coefficient, which is related to the relaxation rate of long-wavelength perturbations [11], characterizes density relaxation in the

---

*[*]tanmoy.chakraborty@bose.res.in
[†]punyabrata.pradhan@bose.res.in*

system. In principle, the bulk-diffusion coefficient should be distinguished from the self-diffusion coefficient of a tagged particle [12–14]; however, the distinction, which can be quite striking, particularly in one-dimensional models [15,16], is somewhat less emphasized in the context of active matter systems [17,18]. In our recent work [14], we considered two models of athermal hardcore RTPs, for which we explicitly calculated the bulk-diffusion coefficient and characterized density relaxation in the system for arbitrary parameter values. However, the other transport coefficient—the collective particle mobility, which is directly connected to the fluctuation of the space-time integrated current over the entire system [19]— is much less explored for interacting SPPs and is studied here for the same models considered in Ref. [14]. It is important to note that the space-time integrated current is nothing but the *cumulative* displacement of all (tagged) particles in a given direction up to certain time. Of course, the knowledge of only the mean squared displacement (MSD) of a *single* tagged particle is not enough to calculate the collective particle mobility, which essentially involves many-particle correlations (over all tagged particles). Indeed, one of the primary objectives of this work is to theoretically characterize of the mobility by calculating the space-time integrated current fluctuations. Another goal is to understand the spatial correlations of (appropriately coarse-grained) current or, equivalently, "velocity," which has recently received significant attention in the contexts of coarsening in the Vicsek model [20], ordering dynamics in the ABPs [21–24], and other active matter systems [25–28].

In the past decades, several analytical studies of current fluctuations for passive lattice gases have been conducted using microscopic [29–33] as well as hydrodynamic frameworks [19,34,35]. However, their extension to interacting SPPs is still a work in progress. In fact, unlike studies of tagged particle displacement fluctuations [36–39], there are few studies of current fluctuations in conventional models of SPPs, with the exception of an exact analysis for noninteracting RTPs [40] and an approximate analysis for ABPs [41]. Recently, exact studies of fluctuations in "weakly interacting" RTPs [42], which are governed by mean-field hydrodynamics, were carried out in Refs. [43–45]. While weakly interacting RTPs undergo diffusion (symmetric hopping) with a *finite* rate, run-and-tumble dynamics on the other hand occur with vanishingly small *system-size-dependent* rates, thus distinguishing the model from the conventional or the standard ones [46,47]. Indeed, in the latter models, the hopping dynamics is independent of system size; as a result, spatial correlations are finite, and long-ranged for small tumbling rates. In such a case, the mean-field description of Refs. [42,43] would not be applicable and a detailed microscopic study of the conventional, "strongly interacting," RTPs is desirable.

In this paper, we use a microscopic approach to investigate spatiotemporal correlations of current in two models of strongly interacting athermal RTPs: model I, standard hardcore RTPs, and model II, a hardcore long-ranged lattice gas (LLG), which is an analytically tractable idealized variant of model I [14]. We study the models on a one-dimensional ring of L sites for arbitrary tumbling rate $\gamma = \tau_p^{-1}$ and density ρ. Interestingly, despite having nontrivial many-body correlations, model II is amenable to "first-principles" analytical calculations, whereas model I is studied through Monte

Carlo simulations. We demonstrate that large-scale fluctuations in both models can be characterized in terms of the two density- and tumbling-rate-dependent transport coefficients: the bulk-diffusion coefficient $D(\rho, \gamma)$ and the collective particle mobility $\chi(\rho, \gamma)$. Indeed, the current fluctuations and the mobility in model II are calculated exactly within a previously introduced truncation scheme of Ref. [16], and are expressed in terms of the distribution of gaps between two consecutive particles. For convenience, we provide below a summary of our main findings.

Spatial correlations of current. We calculate the steady-state spatial correlation function $C_r^{JJ} = \lim_{t \to \infty} \langle J_0(t) J_r(t) \rangle$ evaluated at two spatial points separated by distance r, with $J_i(t)$ being instantaneous current across bond $(i, i+1)$ at time t. The correlation functions are shown to decay exponentially, $C_r^{JJ} \sim \exp(-r/\xi)$; the correlation length $\xi(\rho, \gamma)$ is analytically calculated for LLG, with $\xi \sim \sqrt{\tau_p}$ diverging with persistence time τ_p, thus providing a theoretical explanation of the findings in recent simulations and experiments [21,27].

Space-time integrated current fluctuations. We calculate fluctuations of space-time integrated current $Q_{tot} = \sum_{i=1}^{L} Q_i(T)$ or, equivalently, the cumulative displacement of all particles, during time interval T; here $Q_i(T) = \int_t^{t+T} dt J_i(t)$ is the cumulative bond current across the ith bond $(i, i+1)$ during time T. We then study the collective *mobility* $\chi(\rho, \gamma) \equiv \lim_{L \to \infty} (1/2LT) \langle Q_{tot}^2 \rangle$, which, in the limit of $\rho, \gamma \to 0$, obeys a scaling law: the scaled mobility $\gamma^a \chi(\rho, \gamma)/\chi^{(0)}$ as a function of scaled variable $\psi = \rho/\gamma$ is expressed through a scaling function $\mathcal{H}(\psi)$; here $a = 1$ and 2 in models I and II, respectively, and $\chi^{(0)} = \rho(1 - \rho)$ is the mobility in the limiting case of a symmetric simple exclusion process (SSEP) [19]. The scaling function for the LLG is calculated analytically and, in the limit of strong persistence $\psi \gg 1$, it is shown to have an asymptotic behavior $\mathcal{H}(\psi) \sim \psi^{-3/2}$.

Time-integrated bond-current fluctuations. Depending on the density- and tumbling-rate-dependent collective- or bulk-diffusion coefficient $D(\rho, \gamma)$ and system size L, we find three distinct time regimes for the fluctuations of time-integrated bond current $Q_i(T)$:

(i) Initial-time regime $T \ll r_0^2/D$ (where r_0 is the particle diameter, taken to be unity throughout): The bond-current fluctuation $\langle Q_i^2 \rangle (T, L)$ depends on the details of dynamical rules. It exhibits linear (diffusive) growth for model II (LLG), whereas, for model I (standard RTPs), it crosses over from a mildly superdiffusive to a diffusive growth as tumbling rate increases.

(ii) Intermediate-time regime $r_0^2/D \ll T \ll L^2/D$: The current fluctuation displays subdiffusive growth $\langle Q_i^2 \rangle \sim \sqrt{T}$.

(iii) Long-time regime $L^2/D \ll T$: The bond-current fluctuation $\langle Q_i^2 \rangle \sim T$ grows diffusively (linear growth).

So the qualitative behavior in regimes (ii) and (iii) is *universal*, being independent of dynamical rules of the models, though the prefactors in the growth laws are model dependent.

Universal scaling of bond-current fluctuations. Remarkably, in the limit of $L, T \to \infty$ with scaled time $y = DT/L^2$ fixed and regardless of the dynamical rules of the models, the above-mentioned behavior can be succinctly expressed through a *universal* scaling law for the scaled bond-current

fluctuation $D(\rho, \gamma)\langle Q_i^2(T, L)\rangle/2\chi L \equiv \mathcal{W}(y)$ as a function of $y = DT/L^2$ [see Eq. (85)]. For model II (LLG), the scaling function $\mathcal{W}(y)$ is calculated exactly within the truncation scheme.

Dynamic correlations of current. We also calculate, numerically for model I (standard RTPs) and analytically for model II (LLG), the two-point dynamic correlation function $\mathcal{C}_0^{JJ}(t) = \langle J_i(0)J_i(t)\rangle$ for instantaneous current $J_i(t)$. For model II, by using our microscopic dynamical calculations, we derive, at large times, the dynamic correlation function $\mathcal{C}_0^{JJ}(t) \sim -t^{-3/2}$, which is shown to have a long-time power-law tail, with the correlations actually being *negative*.

The paper is organized as follows: In Sec. II, we introduce two models of hardcore RTPs in one dimension. In Sec. III A we describe the procedure for decomposing current into "slow" (diffusive) and "fast" (noiselike) components. Then in Sec. III B, we introduce a truncation scheme, which allows us to calculate spatiotemporal correlations of time-integrated currents. In Secs. III C and III D, we investigate spatiotemporal correlations of instantaneous and fluctuating currents, respectively. Next, in Sec. III E, we characterize fluctuations of total current, leading to the characterization of the collective particle mobility $\chi(\rho, \gamma)$; here we also discuss a scaling law, which is satisfied by the mobility in the limit of strong persistence and small density. In Sec. III F, we characterize bond-current fluctuation and find another scaling law, satisfied by the bond current; the scaling function is found to be the same for both models. Finally, we summarize the paper in Sec. IV with some concluding remarks.

II. MODEL DESCRIPTION

We consider two minimal models of athermal hardcore RTPs on a one-dimensional periodic lattice of L sites where the number of particles, N, is conserved with density $\rho = N/L$. In both the models, particles obey a hardcore constraint; i.e., a site can be occupied by at most one particle and also the crossing between particles is not allowed. We denote the occupation variable $\eta_i = 1$ or 0, depending on whether the site is occupied or not, respectively.

A. Model I: Standard hardcore RTPs

We consider standard hardcore RTPs (see the schematic diagram in the top panel of Fig. 1), previously introduced in Ref. [47]. In this model, in addition to the occupation variable, a spin $s = \pm 1$ is assigned to each particle, with $s = 1$ and $s = -1$ representing its rightward and leftward orientations, respectively. The continuous-time stochastic dynamics are specified below.

(a) *Run:* With unit rate, a particle hops, along its spin direction, to its nearest neighbor provided that the destination site is vacant.

(b) *Tumble:* With rate $\gamma = \tau_p^{-1}$, a particle flips its spin orientation, $s \to -s$.

Clearly, particles retain their spin orientation over a timescale called the persistence time τ_p and, during this time, they exhibit ballistic motion having a constant speed v along the vacant stretch available in the direction of its spin [note that $v = 1$, set by rule (a)].
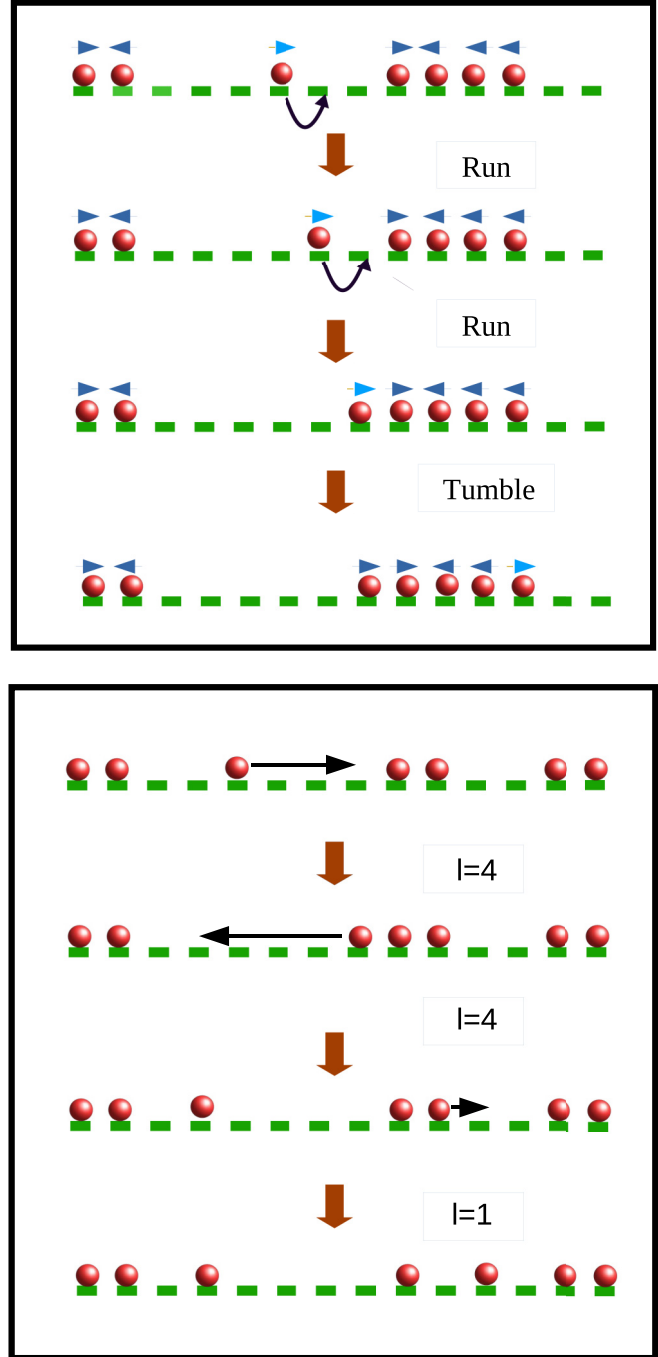

FIG. 1. Schematic diagram of models I and II. Top: Typical microscopic dynamics in model I, which is composed of standard hardcore RTPs (red circles) on a one-dimensional lattice (green rectangles). RTPs move along the associated spin indicated by the arrows above them. Bottom: We demonstrate microscopic dynamics of hardcore particles (red circle) in model II (i.e., LLG) on a one-dimensional lattice (green rectangle). Particles hop symmetrically by length l, which is drawn from an exponential distribution $\phi(l) \sim e^{-l/l_p}$ with integer $l = 0, 1, 2, \ldots$. This particular diagram has been taken from our previous work [14].

B. Model II: Hardcore long-ranged lattice gas

Because of the additional spin degree of freedom, model I is difficult to deal with analytically. To address the issue, we

introduce a simpler idealized variant of hardcore RTPs, called a long-ranged lattice gas (LLG) [14,48], which is amenable to analytical studies. The (athermal) long-range hopping mimics the ballistic motion ("run") of individual RTPs, having a characteristic run length, which is the *persistence length* $l_p = v/\gamma$. Indeed, model II (LLG) is motivated by the fact that, on the timescale of persistence time τ_p, a single RTP would hop, on average, by the typical length l_p.

The precise dynamical rules of model II (see the schematic diagram in the bottom panel of Fig. 1) are as follows. With unit rate, a particle attempts to hop symmetrically by length l, drawn from an exponential distribution $\phi(l)$. The hop is successful provided that, along the hopping direction, there is a vacant stretch, called a gap, of size g, which is of at least size l (i.e., $g \geqslant l$); otherwise (i.e., for $g < l$), due to the hardcore constraint, the particle traverses the entire stretch and sits adjacent to its nearest occupied site. The hop-length distribution $\phi(l)$ can, in principle, be arbitrary. However, to compare the two models I and II, we chose $\phi(l)$ to be an exponential function,

$$\phi(l) = A \exp(-l/l_p), \qquad (2)$$

where the normalization constant $A = (1 - e^{-1/l_p})$ as hop lengths $l = 0, 1, 2, \ldots$ are discrete.

III. THEORY: MODEL II

In this section, we develop a microscopic theoretical framework to analytically calculate current fluctuations in model II (hardcore LLG). We also compare our analytic results with those obtained from direct Monte Carlo simulations of both models I and II.

A. Decomposition of current: Slow and fast components

To begin with, we first define cumulative (time-integrated) bond current $Q_i(T)$, which is the total current across a bond $(i, i+1)$ in a time interval T. On the other hand, instantaneous current $J_i(t)$ is defined as

$$J_i(t) \equiv \lim_{\Delta t \to 0} \frac{\Delta Q_i}{\Delta t}, \qquad (3)$$

where $\Delta Q_i = \int_t^{t+\Delta t} dt J_i(t)$ is the cumulative bond current in time interval Δt. Note that, while we investigate fluctuation properties of both quantities $Q_i(t)$ and $J_i(t)$, in simulations it is statistically more efficient to calculate the averages related to the time-integrated current $Q_i(t)$ than the instantaneous one $J_i(t)$.

However, before discussing the second moment (fluctuations) of currents, in this section, we first investigate their average behavior and set the notations required in the subsequent part of the paper. To this end, let us define the following stochastic variables:

$$\mathcal{U}_{i+l}^{(l)} \equiv \overline{\eta}_{i+1} \overline{\eta}_{i+2} \cdots \overline{\eta}_{i+l}, \qquad (4)$$

$$\mathcal{V}_{i+l+1}^{(l+2)} \equiv \eta_i \overline{\eta}_{i+1} \overline{\eta}_{i+2} \cdots \overline{\eta}_{i+l} \eta_{i+l+1}, \qquad (5)$$

where $\bar{\eta}_i = (1 - \eta_i)$, and $\mathcal{U}^{(l)}$ and $\mathcal{V}^{(l+2)}$ are indicator functions for a single site being vacant, l consecutive sites being vacant, and a vacancy cluster to be of size l, respectively.

Note that, whenever a particle performs a long-range hop of length l, it contributes a unit current at each bond in the stretch between the departure and destination sites; that is, for a rightward (leftward) hop, current across *all* bonds in that stretch increases (decreases) by unity. By considering this, the continuous-time evolution for time-integrated current $Q_i(t)$ in an infinitesimal time interval $[t, t + dt]$ can be written as

$$Q_i(t + dt) = \begin{cases} Q_i(t) + 1, & \text{prob.} \quad \mathcal{P}_i^R(t)dt \\ Q_i(t) - 1, & \text{prob.} \quad \mathcal{P}_i^L(t)dt \\ Q_i(t), & \text{prob.} \quad 1 - \left(\mathcal{P}_i^R + \mathcal{P}_i^L\right)dt, \end{cases} \qquad (6)$$

where $\mathcal{P}_i^R dt$ and $\mathcal{P}_i^L dt$ are probabilities of the hopping events and the corresponding rates are given by [14]

$$\mathcal{P}_i^R \equiv \frac{1}{2} \sum_{l=1}^{\infty} \phi(l) \left[\sum_{k=1}^{l} \left(\mathcal{U}_{i+k}^{(l)} - \mathcal{U}_{i+k}^{(l+1)} \right) + \sum_{g=1}^{l-1} \sum_{k=1}^{g} \mathcal{V}_{i+k+1}^{(g+2)} \right], \qquad (7)$$

$$\mathcal{P}_i^L \equiv \frac{1}{2} \sum_{l=1}^{\infty} \phi(l) \left[\sum_{k=1}^{l} \left(\mathcal{U}_{i+k-1}^{(l)} - \mathcal{U}_{i+k}^{(l+1)} \right) + \sum_{g=1}^{l-1} \sum_{k=1}^{g} \mathcal{V}_{i+k}^{(g+2)} \right]. \qquad (8)$$

By using the above microscopic update rules and doing some straightforward algebraic manipulations, the average instantaneous current $\langle J_i(t) \rangle$ can be written as [14]

$$\langle J_i(t) \rangle = \frac{1}{2} \sum_{l=1}^{\infty} \phi(l) \left[\sum_{g=1}^{l-1} \left(\langle \mathcal{V}_{i+g+1}^{(g+2)} \rangle - \langle \mathcal{V}_{i+1}^{(g+2)} \rangle \right) \right. $$
$$\left. + \left(\langle \mathcal{U}_{i+l}^{(l)} \rangle - \langle \mathcal{U}_i^{(l)} \rangle \right) \right]. \qquad (9)$$

Note that, in the above equation, the average current $\langle J_i(t) \rangle$ is written as a (generalized) gradient of the observables $\langle \mathcal{V}^{(g+2)} \rangle(\rho)$ and $\langle \mathcal{U}^{(l)} \rangle(\rho)$, both of which depend on (local) density and, of course, tumbling rate. By making use of Taylor's expansion, we can write the average current explicitly in terms of (discrete) gradient of (local) density [14],

$$\langle J_i(t) \rangle \simeq -D(\rho, \gamma)[\langle \eta_{i+1}(t) \rangle - \langle \eta_i(t) \rangle], \qquad (10)$$

where $\rho_i(t) = \langle \eta_i(t) \rangle$ is the local density and the bulk-diffusion coefficient $D(\rho, \gamma)$ [14],

$$D(\rho, \gamma) = -\frac{1}{2} \sum_{l=1}^{\infty} \phi(l) \frac{\partial}{\partial \rho} \left[\sum_{g=1}^{l-1} g \langle \mathcal{V}^{(g+2)} \rangle(\rho) + l \langle \mathcal{U}^{(l)} \rangle(\rho) \right], \qquad (11)$$

is a function of the global density ρ and tumbling rate γ. As shown in Ref. [14], the correlation functions $\langle \mathcal{V}^{(g+2)} \rangle$ and $\langle \mathcal{U}^{(l)} \rangle$, and therefore the bulk-diffusion coefficient $D(\rho, \gamma)$, can be written in terms of the gap distribution $P(g)$ by using

the following relations:

$$\langle \mathcal{V}^{(g+2)}(\rho, \gamma) \rangle = \rho P(g), \tag{12}$$

$$\langle \mathcal{U}^{(l)}(\rho, \gamma) \rangle = \rho \sum_{g=l-1}^{\infty} (g - l + 1)P(g). \tag{13}$$

Then the resulting expression of the bulk-diffusion coefficient $D(\rho, \gamma)$ is given by [14]

$$D(\rho, \gamma) = -\frac{1}{2} \frac{\partial}{\partial \rho} \left[\rho \sum_{l=1}^{\infty} \phi(l) \left(\sum_{g=1}^{l-1} gP(g) + l \sum_{g=l-1}^{\infty} (g - l + 1)P(g) \right) \right], \tag{14}$$

which will be required later to explicitly calculate the current fluctuations in the system.

As the system is homogeneous in the steady state, the gradients in Eq. (9) simply vanish, implying that the system has *zero* steady-state current. However, on the level of fluctuations, the (stochastic) instantaneous current is in fact *nonzero* even in the steady state. To characterize fluctuations appropriately [10,19], we decompose the total instantaneous current into two components: a (hydrodynamic) diffusive current $J_i^{(D)}$, which relaxes very slowly, and a fluctuating or noise current $J_i^{(fl)}$, which is then expected to relax fast. In other words, we write the instantaneous current as the sum of these slow and fast components,

$$J_i(t) = J_i^{(D)}(t) + J_i^{(fl)}(t), \tag{15}$$

where we identify, by using Eq. (9), the diffusive current

$$J_i^{(D)} \equiv \frac{1}{2} \sum_{l=1}^{\infty} \phi(l) \left[\sum_{g=1}^{l-1} \left(\mathcal{V}_{i+g+1}^{(g+2)} - \mathcal{V}_{i+1}^{(g+2)} \right) + \left(\mathcal{U}_{i+l}^{(l)} - \mathcal{U}_i^{(l)} \right) \right]. \tag{16}$$

Indeed, as we derive later [see Eqs. (60) and (67)], the time-dependent correlation function for the diffusive current $J_i^{(D)}$ (also the total current J_i) has a power-law tail, whereas that for the fluctuating (noise) current $J_i^{(fl)}$ is delta correlated. Also, by comparing Eqs. (9), (15), and (16), we find that the average fluctuating current is simply zero:

$$\langle J_i^{fl}(t) \rangle = 0. \tag{17}$$

However, the space-time correlations of J_i^{fl} have nontrivial spatial structures [see Eq. (67)]. In the subsequent section, these spatiotemporal correlations are analytically calculated by using a truncation scheme, which we discuss next.

B. Spatiotemporal correlations of current

We consider time-integrated currents $Q_r(t')$ and $Q_0(t)$, which are measured up to times t' and t ($t' > t$) across bonds $(r, r+1)$ and $(0, 1)$, respectively, with the bonds being spatially separated by distance r. In this section, we investigate the space-time-dependent correlation function for bond current $Q_i(t)$,

$$\mathcal{C}_r^{QQ}(t', t) = \langle Q_r(t') Q_0(t) \rangle_c$$
$$= \langle Q_r(t') Q_0(t) \rangle - \langle Q_r(t') \rangle \langle Q_0(t) \rangle. \tag{18}$$

As we choose $t' > t$, it is easy to see that, in an infinitesimal time interval $[t', t' + dt']$, $Q_0(t)$ remains constant, and any change in $\mathcal{C}_r^{QQ}(t', t)$ occurs solely due to the change in

$Q_r(t')$. Now, by using infinitesimal update rules [Eq. (6)], we write down the time-evolution equation for $\mathcal{C}_r^{QQ}(t', t)$ as given below (see Appendix A for details):

$$\frac{d}{dt'} \mathcal{C}_r^{QQ}(t', t) = \frac{1}{2} \sum_{l=1}^{\infty} \phi(l) \left[\left\{ \mathcal{C}_{r+l}^{\mathcal{U}^{(l)}Q}(t', t) - \mathcal{C}_r^{\mathcal{U}^{(l)}Q}(t', t) \right\} \right.$$
$$\left. + \sum_{g=1}^{l-1} \left\{ \mathcal{C}_{r+g+1}^{\mathcal{V}^{(g+2)}Q}(t', t) - \mathcal{C}_{r+1}^{\mathcal{V}^{(g+2)}Q}(t', t) \right\} \right]. \tag{19}$$

In other words, we have the following identity:

$$\frac{d}{dt'} \mathcal{C}_r^{QQ}(t', t) = \langle J_r^{(D)}(t') Q_0(t) \rangle_c, \tag{20}$$

where $J_r^{(D)}(t)$ is the diffusive current across the rth bond and at time t. Note that Eq. (19) for two-point current correlation is exact and has been expressed as the gradients of two nontrivial multipoint correlation functions,

$$\mathcal{C}_r^{\mathcal{U}^{(l)}Q}(t', t) = \langle \mathcal{U}_r^{(l)}(t') Q_0(t) \rangle_c, \tag{21}$$

$$\mathcal{C}_r^{\mathcal{V}^{(g+2)}Q}(t', t) = \langle \mathcal{V}_r^{(g+2)}(t') Q_0(t) \rangle_c. \tag{22}$$

However, the difficulty arises here because the two-point correlation in Eq. (19) involves various multipoint correlation functions, which must now be calculated in order to determine $\mathcal{C}_r^{QQ}(t', t)$. Not surprisingly, the hierarchy involving the time evolution of $\mathcal{C}_r^{\mathcal{U}^{(l)}Q}(t', t)$ and $\mathcal{C}_r^{\mathcal{V}^{(g+2)}Q}(t', t)$ does not close, making exact calculations quite difficult.

To address the above-mentioned difficulty, in this paper, we now use a truncation scheme that, though approximate, allows us to close the above hierarchy and to write the time evolution of the two-point current correlations in terms of two-point correlations, involving only current and density, which, interestingly, close onto themselves. Indeed, when fluctuations of local density around the steady state are small, on a long timescale the variables $\mathcal{V}^{(g+2)}$ and $\mathcal{U}^{(l)}$ appearing in Eq. (16) are essentially "slaved" to local density and, as a result, the diffusive current could be approximately written in the form of a "microscopic" version of Fick's law [33], which is evident from Eq. (10):

$$J_r^{(D)}(t') \simeq D(\rho, \gamma)[\eta_r(t') - \eta_{r+1}(t')]. \tag{23}$$

Here we have simply used $D[\rho_r(t), \gamma] \simeq D(\rho, \gamma)$; the symbol "$\simeq$" in Eq. (23) should rather be interpreted as an "equivalence," not an "equality," between the random variables there, unless one takes explicit averages. The precise implication of

the above equivalence relation in Eq. (23), which has been used in the subsequent calculations, is the following: We simply write the correlation function for diffusive current $J_r^{(D)}(t')$ and any other stochastic variable $B(t)$ in terms of correlations between local density and the variable $B(t)$, i.e.,

$$\left\langle J_r^{(D)}(t')B(t)\right\rangle_c \simeq -D(\rho,\gamma)\Delta_r\langle\eta_r(t')B(t)\rangle_c, \quad (24)$$

where $\Delta_r h_r = h_{r+1} - h_r$ is the forward difference operator. Following the above truncation scheme [Eq. (24)], the time evolution of the current correlations in Eq. (20) greatly simplifies as the gradient of two-point density-current correlation function $\mathcal{C}_r^{\eta Q}(t',t) = \langle\eta_r(t')Q_0(t)\rangle_c$, which, as shown below, immediately closes the hierarchy. We thus rewrite Eq. (20) as

$$\frac{d}{dt'}\mathcal{C}_r^{QQ}(t',t) \simeq -D(\rho,\gamma)\Delta_r\mathcal{C}_r^{\eta Q}(t',t), \quad (25)$$

whereas the time evolution of the density-current correlation $\mathcal{C}_r^{\eta Q}(t',t)$ can be written as (for details see Appendix B)

$$\frac{d}{dt'}\mathcal{C}_r^{\eta Q}(t',t) = D(\rho,\gamma)\Delta_r^2\mathcal{C}_r^{\eta Q}(t',t). \quad (26)$$

Notably, the SSEP, despite having a product-measure steady state and the bulk-diffusion coefficient being independent of density [33], shares a quite similar structure involving the density and current correlations, which, for LLG, however, require calculations of various nontrivial spatiotemporal correlations. To further simplify the time-evolution equations governing the two-point correlations, we represent the correlation functions in the Fourier space by using the transformation

$$\tilde{\mathcal{C}}_q^{AB}(t',t) = \sum_{r=0}^{L-1}\mathcal{C}_r^{AB}(t',t)e^{iqr}. \quad (27)$$

The inverse Fourier transform is given by

$$\mathcal{C}_r^{AB}(t',t) = \frac{1}{L}\sum_q\tilde{\mathcal{C}}_q^{AB}(t',t)e^{-iqr}, \quad (28)$$

where

$$q = \frac{2\pi n}{L}, \quad (29)$$

and $n = 0, 1, 2, \ldots, (L-1)$. We rewrite Eqs. (25) and (26) in terms of the time evolution of the respective Fourier modes,

$$\frac{d}{dt'}\tilde{\mathcal{C}}_q^{QQ}(t',t) = D(\rho,\gamma)(1-e^{-iq})\tilde{\mathcal{C}}_q^{QQ}(t',t) \quad (30)$$

and

$$\frac{d}{dt'}\tilde{\mathcal{C}}_q^{\eta Q}(t',t) = -D(\rho,\gamma)\lambda_q\tilde{\mathcal{C}}_q^{\eta Q}(t',t), \quad (31)$$

where λ_q is given by

$$\lambda_q = 2(1-\cos q). \quad (32)$$

By integrating Eqs. (30) and (31), we express the unequal-time correlation functions in the following forms:

$$\tilde{\mathcal{C}}_q^{QQ}(t',t) = D(\rho,\gamma)\int_t^{t'}dt''(1-e^{-iq})\tilde{\mathcal{C}}_q^{\eta Q}(t'',t)+\tilde{\mathcal{C}}_q^{QQ}(t,t), \quad (33)$$

$$\tilde{\mathcal{C}}_q^{\eta Q}(t'',t) = e^{-\lambda_q D(\rho,\gamma)(t''-t)}\tilde{\mathcal{C}}_q^{\eta Q}(t,t), \quad (34)$$

where $t'' \geqslant t$. It is now clear that, to evaluate the unequal-time correlation functions, $\mathcal{C}_r^{QQ}(t',t)$ and $\mathcal{C}_r^{\eta Q}(t',t)$, one must first calculate their equal-time counterparts, which we do next.

1. Equal-time density-current correlation $\tilde{\mathcal{C}}_q^{\eta Q}(t,t)$

We have already seen in Eq. (33) that the density-current correlation function $\tilde{\mathcal{C}}_q^{\eta Q}$ plays an important role in determining $\tilde{\mathcal{C}}_q^{QQ}$. We therefore proceed with the calculation of the equal-time density-current correlation function $\tilde{\mathcal{C}}_q^{\eta Q}(t,t)$ (for details of the following calculations, see Appendix C). Starting from microscopic dynamical rules, we obtain the time evolution of $\mathcal{C}_r^{\eta Q}(t,t)$, which, in terms of the Fourier modes, satisfies the following equation:

$$\left(\frac{d}{dt}+D(\rho,\gamma)\lambda_q\right)\tilde{\mathcal{C}}_q^{\eta Q}(t,t) = \tilde{\mathcal{S}}_q^{\eta Q}(t). \quad (35)$$

Here the source term $\tilde{\mathcal{S}}_q^{\eta Q}(t)$ is given by

$$\tilde{\mathcal{S}}_q^{\eta Q}(t) = \frac{1}{(1-e^{-iq})}\left[D(\rho,\gamma)\lambda_q\tilde{\mathcal{C}}_q^{\eta\eta}(t,t)-f_q(t)\right], \quad (36)$$

where $f_q(t)$ is directly related to the gap distribution $P(g,t)$ of the system and is given by

$$f_q(t) = \rho\sum_{l=1}^{\infty}\phi(l)\left[\sum_{g=1}^{l-1}\lambda_{gq}P(g,t)+\lambda_{lq}\sum_{g=l}^{\infty}P(g,t)\right]. \quad (37)$$

We can now solve for $\tilde{\mathcal{C}}_q^{\eta Q}(t,t)$ by integrating Eq. (35) and the solution is given by

$$\tilde{\mathcal{C}}_q^{\eta Q}(t,t) = \int_0^t dt'''e^{-\lambda_q D(\rho,\gamma)(t-t''')}\tilde{\mathcal{S}}_q^{\eta Q}(t'''), \quad (38)$$

which, upon substitution in Eq. (34), leads to the unequal-time density-current correlation function,

$$\tilde{\mathcal{C}}_q^{\eta Q}(t'',t) = \int_0^t dt'''e^{-\lambda_q D(\rho,\gamma)(t''-t''')}\tilde{\mathcal{S}}_q^{\eta Q}(t'''). \quad (39)$$

Note that, in the above analysis, $\tilde{\mathcal{S}}_q^{\eta Q}(t)$ and hence $\tilde{\mathcal{C}}_q^{\eta Q}(t,t)$ and $\tilde{\mathcal{C}}_q^{\eta Q}(t'',t)$ have been expressed in terms of the equal-time density-density correlation function $\tilde{\mathcal{C}}_q^{\eta\eta}(t,t)$, which remains to be the only unknown quantity so far and has to be determined. To this end, we first derive the time-evolution equation for the correlation function $\mathcal{C}_r^{\eta\eta}(t,t) = \langle\eta_r(t)\eta_0(t)\rangle_c$, in the real space (for details, see Appendix D). Using a Fourier transform of Eq. (27), we find the time-evolution equation for Fourier modes $\tilde{\mathcal{C}}_q^{\eta\eta}(t,t)$,

$$\left(\frac{d}{dt}+2D(\rho,\gamma)\lambda_q\right)\tilde{\mathcal{C}}_q^{\eta\eta}(t,t) = \tilde{\mathcal{S}}_q^{\eta\eta}(t), \quad (40)$$

where the source term $\tilde{\mathcal{S}}_q^{\eta\eta} = f_q$. One can now solve Eq. (40) to obtain the time-dependent solution of $\tilde{\mathcal{C}}_q^{\eta\eta}(t,t)$. Since we want the dynamic density-density correlation function to be evaluated in the steady state, we simply drop its time dependence and set $d\tilde{\mathcal{C}}_q^{\eta\eta}(t,t)/dt = 0$; consequently, we have from Eq. (40)

$$2D(\rho,\gamma)\lambda_q\tilde{\mathcal{C}}_q^{\eta\eta} = \tilde{\mathcal{S}}_q^{\eta\eta} = f_q. \quad (41)$$

Equation (41) provides the solution for the static density-density correlation function and f_q is then obtained by replacing $P(g, t)$ by its steady-state value $P(g)$ in Eq. (37). Upon substituting the static $\tilde{\mathcal{C}}_q^{\eta\eta}$ in Eq. (36), the source term $\tilde{\mathcal{S}}_q^{\eta Q}$ also becomes time independent and thus the solution is given by

$$\tilde{\mathcal{S}}_q^{\eta Q} = -\frac{f_q}{2(1 - e^{-iq})}. \quad (42)$$

Using this particular form of $\tilde{\mathcal{S}}_q^{\eta Q}$ in Eq. (39), we finally obtain the equal- as well as unequal-time density-current correlation function $\tilde{\mathcal{C}}_q^{\eta Q}$ in the steady state,

$$\tilde{\mathcal{C}}_q^{\eta Q}(t, t) = \frac{-f_q}{2D(\rho, \gamma)\lambda_q(1 - e^{-iq})}\left(1 - e^{-\lambda_q D(\rho, \gamma)t}\right), \quad (43)$$

$$\tilde{\mathcal{C}}_q^{\eta Q}(t'', t) = \frac{-f_q e^{-\lambda_q D(\rho, \gamma)t''}}{2D(\rho, \gamma)\lambda_q(1 - e^{-iq})}\left(e^{\lambda_q D(\rho, \gamma)t} - 1\right), \quad (44)$$

where $t'' \geqslant t$. It should be noted that, by substituting Eq. (44) in Eq. (33), one can readily obtain the first term of the unequal-time current-current correlation function $\tilde{\mathcal{C}}_q^{QQ}(t'', t)$. In the next section, we focus on another equal-time correlation function $\mathcal{C}_r^{QQ}(t, t)$, which is the quantity to be considered while calculating the two-point space-time correlation function $\mathcal{C}_r^{QQ}(t', t)$.

2. Equal-time current-current correlation $\mathcal{C}_r^{QQ}(t, t)$

To calculate the equal-time current-current correlation $\mathcal{C}_r^{QQ}(t, t)$, we first derive its time-evolution equation, which, upon applying the closure scheme as in Eq. (23), leads to the solution for $\mathcal{C}_r^{QQ}(t, t)$ having the following closed-form expression:

$$\mathcal{C}_r^{QQ}(t, t) = \frac{D}{L}\sum_q(1 - e^{-iq})(2 - \lambda_{qr})\int_0^t \tilde{\mathcal{C}}_q^{\eta Q}(t, t)dt + \Gamma_r t. \quad (45)$$

On the right-hand side of the above equation, $\tilde{\mathcal{C}}_q^{\eta Q}(t, t)$ in the first term is readily obtained from Eq. (43), while, in the

second term, Γ_r can be written in terms of gap distribution as given below:

$$\Gamma_r = \rho \sum_{l=|r|+1}^{\infty} \phi(l)\left[(l - |r|)\sum_{g=l}^{\infty} P(g) + \sum_{g=|r|}^{l-1}(g - |r|)P(g)\right] \quad (46)$$

(see Appendix E for calculation details). The quantity Γ_r physically corresponds to the strength of the "noise current" and is shown to be equal to the two-point space-time correlation of the fluctuating current, i.e., $\langle J_r^{(fl)}(t)J_0^{(fl)}(0)\rangle = \Gamma_r \delta(t)$ [see Eq. (67)]. Later we also show that the steady-state fluctuation of the space-time integrated current $Q_{\text{tot}}(L, T) = \int_0^T dt \sum_{i=0}^{L-1} J_i^{(fl)}(t)$ [see Eq. (74)] satisfies, in the thermodynamic limit, a fluctuation relation,

$$2\chi(\rho, \gamma) \equiv \lim_{L \to \infty}\frac{1}{LT}\langle Q_{\text{tot}}^2(L, T)\rangle = \sum_r \Gamma_r, \quad (47)$$

where the particle mobility $\chi(\rho, \gamma)$ has the following expression:

$$\chi(\rho, \gamma) = \frac{\rho}{2}\sum_{l=1}^{\infty}\phi(l)\left[\sum_{g=1}^{l-1} g^2 P(g) + l^2\sum_{g=l}^{\infty} P(g)\right]. \quad (48)$$

The mobility can be written explicitly as a function of density and tumbling rate, provided that the gap distribution $P(g)$ is known (see the $\rho, \gamma \to 0$ limit and the corresponding scaling regime, discussed later in Sec. III E). Note that the sum rule, as in Eq. (47), states that the scaled space-time integrated current fluctuation is equal to the spatially integrated correlation function for fluctuating current and can be directly tested in simulations [see Fig. 4].

We now perform an inverse Fourier transform of Eq. (33) and finally obtain the desired solution for the steady-state unequal-time two-point current-current correlation function $\mathcal{C}_r^{QQ}(t', t)$ in real space,

$$\mathcal{C}_r^{QQ}(t', t) = -\frac{1}{2LD}\sum_q \frac{f_q}{\lambda_q^2}(e^{-\lambda_q Dt} - e^{-\lambda_q Dt'})(e^{-\lambda_q Dt} - 1)e^{-iqr} - \frac{1}{2L}\sum_q \frac{f_q}{\lambda_q}\left\{t - \frac{(1 - e^{-\lambda_q Dt})}{\lambda_q D}\right\}(2 - \lambda_{qr}) + \Gamma_r t. \quad (49)$$

Now onwards, to keep the notations simple, we drop the argument of $D(\rho, \gamma)$ in Eq. (49) and elsewhere.

C. Spatiotemporal correlation of the instantaneous current

In this section, we calculate the two-point unequal-time correlation function of the instantaneous current, i.e., $\mathcal{C}_r^{JJ}(t', t)$ in the steady state. We do this by differentiating the steady-state integrated current correlation function $\mathcal{C}_r^{QQ}(t', t)$ with respect to times t' and t. However, the expression for $\mathcal{C}_r^{QQ}(t', t)$ provided in Eq. (49) is valid only for $t' \geqslant t$. Therefore, to obtain $\mathcal{C}_r^{JJ}(t', t)$ for arbitrary values of t' and t, the appropriate formula can be written by using the Heaviside

theta function $\Theta(t)$,

$$\mathcal{C}_r^{JJ}(t, t') = \frac{d}{dt}\frac{d}{dt'}\left[\mathcal{C}_r^{QQ}(t', t)\Theta(t' - t) + \mathcal{C}_r^{QQ}(t, t')\Theta(t - t')\right], \quad (50)$$

where $\mathcal{C}_r^{QQ}(t, t')$ is obtained directly from Eq. (49) by interchanging t' and t. Using Eq. (50), we straightforwardly compute $\mathcal{C}_r^{JJ}(t', t)$. After doing some algebraic manipulations and setting $t' = 0$, we eventually arrive at the following expression:

$$\mathcal{C}_r^{JJ}(t, t') = \Gamma_r \delta(t - t') - \frac{D}{4L}\sum_q(2 - \lambda_{qr})f_q e^{-\lambda_q D|t - t'|}$$
$$\times \{\Theta(t - t') + \Theta(t' - t)\}, \quad (51)$$

where f_q is obtained by substituting the steady-state gap distribution $P(g)$ in Eq. (37). Clearly, $\mathcal{C}_r^{JJ}(t, t')$ can be divided into two distinct parts. The space-dependent prefactor in the first component, which is delta correlated in time, pertains to the equal-time two-point correlation, which in turn is determined by the fluctuating current correlations Γ_r. The second part comprises the correlations at different space and time points. In the subsequent analysis, we examine the contribution of each of these terms.

1. Equal-time unequal-space correlation

To obtain the equal-time spatial correlations of the instantaneous current, we consider the case in Eq. (51) with $t = t' = 0$, yielding the leading-order contribution,

$$\mathcal{C}_r^{JJ} \simeq \left(\frac{\mathcal{C}_0^{JJ}}{\Gamma_0}\right)\Gamma_r. \tag{52}$$

Note that the spatial dependence of the correlation function $\mathcal{C}_r^{JJ}$ is solely governed by Γ_r, which can be written in terms of the steady-state gap distribution function $P(g)$ only [see Eq. (46)]. So, perhaps not surprisingly, the spatial correlations of current are in fact governed by the gap statistics and one would expect the correlation length to be determined by the typical gap size in the system. However, obtaining $P(g)$ explicitly as a function of ρ and γ is not an easy task in general. We can still do the following asymptotic analysis, which is quite general. For larger gap size, we expect $P(g)$ to be an exponential function (which can be shown to be indeed the case for $\gamma \ll 1$ [49]),

$$P(g) \simeq N_* \exp(-g/g_*), \tag{53}$$

where g_* is the typical gap size. Now, using the conservation relation $\langle g \rangle = \sum_{g=1}^{\infty} g P(g) = 1/\rho - 1$, one can immediately obtain the prefactor

$$N_* \simeq \left(\frac{1}{\rho} - 1\right)\frac{(e^{1/g_*} - 1)^2}{e^{1/g_*}}. \tag{54}$$

Upon substituting the above expression of $P(g)$ into Eq. (46), we obtain the following simplified expression:

$$\Gamma_r \simeq (1 - \rho)\frac{(e^{1/g_*} - 1)}{(e^{(\gamma + 1/g_*)} - 1)}e^{-r/\xi} = \Gamma_0 e^{-r/\xi}. \tag{55}$$

The above equation immediately leads to the spatial correlation function of the current,

$$\mathcal{C}_r^{JJ} = \mathcal{C}_0^{JJ}e^{-r/\xi}, \tag{56}$$

where the correlation length ξ is given by

$$\xi = \frac{1}{\gamma + g_*^{-1}}. \tag{57}$$

Equations (55) and (57) imply that the typical gap size g_* plays a crucial role in determining Γ_r and ξ. Although one can calculate g_* numerically without much difficulty, the determination of its exact analytical form for any arbitrary parameter regime is a nontrivial task. However, in the limit of strong persistence where $l_p = \gamma^{-1} \to \infty$, there is an analytic expression for typical gap size [49],

$$g_* \simeq \sqrt{\frac{1 - \rho}{\gamma\rho}}, \tag{58}$$

which leads to the explicit solution of Γ_r and hence the correlation function C_r^{JJ}. It is worth noting that, in this specific regime of strong persistence, the correlation length ξ is primarily dominated by g_* alone, which immediately implies $\xi \sim 1/\sqrt{\gamma} = \sqrt{\tau_p}$. That is, correlation length $\xi \sim \sqrt{\tau_p}$ diverges with persistence time τ_p, thus providing a straightforward theoretical explanation of the findings in recent simulations and experiments [21,27].

In order to verify the theoretical results in Eqs. (56), (57), and (58), in simulations we actually calculate, for better statistics, correlation function $C^{\bar{J}\bar{J}}(r) = \lim_{t\to\infty}\langle \bar{J}_0(t)\bar{J}_r(t)\rangle$ for a coarse-grained current $\bar{J}_i(t) = (1/\Delta t)\int_t^{t+\Delta t} dt J_i(t)$, averaged over a reasonably small time window $(t, t + \Delta t)$ and evaluated at two spatial points separated by distance r. In Fig. 2, we plot the scaled correlation function $\mathcal{C}_r^{JJ}/\mathcal{C}_0^{JJ}$ for models II (LLG, closed points; left-hand panel) and I (standard RTPs, open points; middle panel), obtained from Monte Carlo simulation, at different tumbling rates $\gamma = 0.05$ (triangle), 0.02 (inverted triangle), 0.01 (diamond), and 0.005 (pentagon) while keeping the density fixed at $\rho = 0.5$. We also compare the simulation data with the strong-persistence analytical solution (dotted lines), obtained using Eqs. (56), (57), and (58). We indeed find quite good agreement between simulations and analytic results in the limit of small γ. Finally, in the right-hand panel of Fig. 2, we plot the numerically obtained correlation length ξ as a function of γ for models II (LLG, closed points) and I (standard RTPs, open points) at a fixed density $\rho = 0.5$ and also compare the results with the strong-persistence analytical solution, obtained using Eqs. (57) and (58). In both cases, models I and II, we find in simulations that the correlation functions decay exponentially, $C^{\bar{J}\bar{J}}(r) \sim \exp(-r/\xi)$, and agree reasonably well with the analytical results. Notably, at small γ, the correlation lengths for models I and II asymptotically converge to each other, as implied by our theory in Eqs. (56), (57), and (58).

2. Equal-space unequal-time correlation function

To evaluate the dynamic two-point correlation function for the instantaneous current in the steady state, we set $r = 0$ and consider the case $t' = 0$ and $t > 0$ in Eq. (51), leading to the following expression:

$$\mathcal{C}_0^{JJ}(t, 0) = -\frac{D}{2L}\sum_q f_q(t)e^{-\lambda_q Dt}. \tag{59}$$

It is important to distinguish between the order of space and time limits. In the case where the long-time limit $t \to \infty$ is taken first and then the large-system-size limit $L \to \infty$ (i.e., $t \gg L^2/D$), it can be shown from Eq. (59) that $\mathcal{C}_0^{JJ}(t, 0) = 0$. In the other case, where we first take the limit $L \to \infty$ and then the $t \to \infty$ limit (i.e., $L^2/D \gg t \gg r_0^2/D$, where r_0 is the lattice spacing, or particle diameter, taken to be unity throughout), we observe that the dynamic correlation $\mathcal{C}_0^{JJ}(t, 0)$ becomes a long-ranged one. In this time regime, the behavior of $\mathcal{C}_0^{JJ}(t, 0)$ in Eq. (59) is primarily dominated by
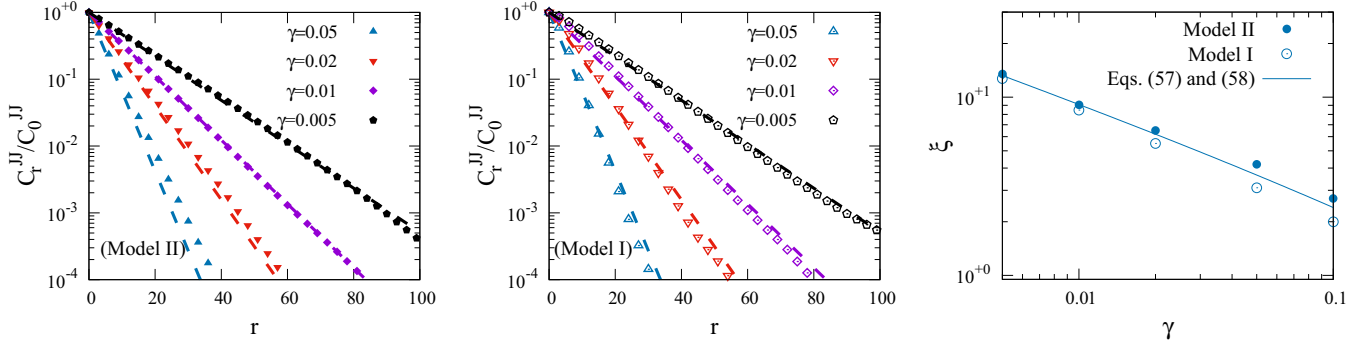
FIG. 2. Verification of Eqs. (56), (57), and (58). We plot the scaled two-point spatial correlation of the instantaneous current $\mathcal{C}_r^{JJ}/\mathcal{C}_0^{JJ}$ for model II (LLG, left-hand panel) and model I (standard RTPs, middle panel), obtained from simulations (points), at a fixed $\rho = 0.5$ and various $\gamma = 0.05$ (triangle), 0.02 (inverted triangle), and 0.01 (diamond). We also compare the simulation data in both models with the strong persistence analytical solution (dotted line) given by Eqs. (56), (57), and (58). In the right-hand panel, we plot the correlation length ξ, as a function of γ, at $\rho = 0.5$ for model II (LLG, closed points) and model I (RTPs, open points) and compare them with the strong persistence analytical solution (line) provided by Eqs. (57) and (58).

the relaxations of the small-q Fourier modes. Therefore, in order to obtain the large-t behavior, we can employ a small-q analysis by performing the transformations $\lambda_q \to q^2$ and $f_q \to \chi(\rho, \gamma)q^2$. Moreover, for large $L \gg 1$, by converting the summation into an integral, we obtain, for large times,

$$\mathcal{C}_0^{JJ}(t) \simeq -\frac{\chi(\rho, \gamma)}{4\sqrt{\pi D(\rho, \gamma)}}t^{-3/2} \qquad (60)$$

(see Appendix F for calculation details). Notably, the correlation function $\mathcal{C}_0^{JJ}(t, 0)$ is *negatively correlated* for $t > 0$, with a delta function at $t = 0$, and exhibits a power-law decay. These two important characteristics are a direct consequence of the observed subdiffusive growth in $\mathcal{C}_0^{QQ}(t, t)$ in the time regime $1 \ll Dt \ll L^2$. In fact, in this regime, upon suitable rearrangements of Eq. (60), we immediately obtain a scaling law,

$$\frac{1}{\chi D}\mathcal{C}_0^{JJ}(t) = -\frac{1}{4\sqrt{\pi}}(Dt)^{-3/2}. \qquad (61)$$

Here $\chi(\rho, \gamma)$ and $D(\rho, \gamma)$ are the density- and tumbling-rate-dependent collective mobility, as in Eq. (48), and bulk-diffusion coefficient, respectively. Interestingly, in a slightly different setting, dynamic fluctuations of "force" on a "passive" tracer immersed in a bath of hardcore RTPs have been studied in Ref. [50], where the associated correlation function was shown to have a similar power-law tail.

In order to verify the scaling law in Eq. (61), we first require to calculate the parameter-dependent transport coefficients $D(\rho, \gamma)$ and $\chi(\rho, \gamma)$ for models I and II. We calculate $D(\rho, \gamma)$ and $\chi(\rho, \gamma)$ for model II (LLG) by numerically computing $P(g)$ in the steady state and then using it in Eqs. (14) and (48), respectively. However, for model I (standard hardcore RTPs), we do not have any analytical expressions for the two transport coefficients and therefore, to explicitly calculate them, we resort to Monte Carlo simulations. To calculate $D(\rho, \gamma)$ for model I, we studied in our previous work [14] relaxation of long-wavelength perturbation through a quite efficient Monte Carlo algorithm. Now, for numerical calculation of the particle mobility $\chi(\rho, \gamma)$, we directly compute the scaled space-time integrated current fluctuation as given in Eq. (74). We now verify Eq. (61) by plotting the

(negative) scaled correlation function $-\mathcal{C}_0^{JJ}(t)/\chi D$ (obtained from simulations) as a function of scaling variable Dt in Fig. 3, for model II (closed points) and model I (open points) for various densities $\rho = 0.3$ (circle), 0.5 (square), and 0.7 (triangle) at a fixed tumbling rate $\gamma = 0.1$. We also compare simulation results (points) with the analytic solution as given in Eq. (61). We find that, at large times, theory agrees quite well with simulations.

D. Space-time correlations of fluctuating ("noise") current

In this section, we focus on determining the two-point spatiotemporal correlation function for fluctuating current $J^{(fl)}(t)$ in the steady state. In other words, we aim to derive the
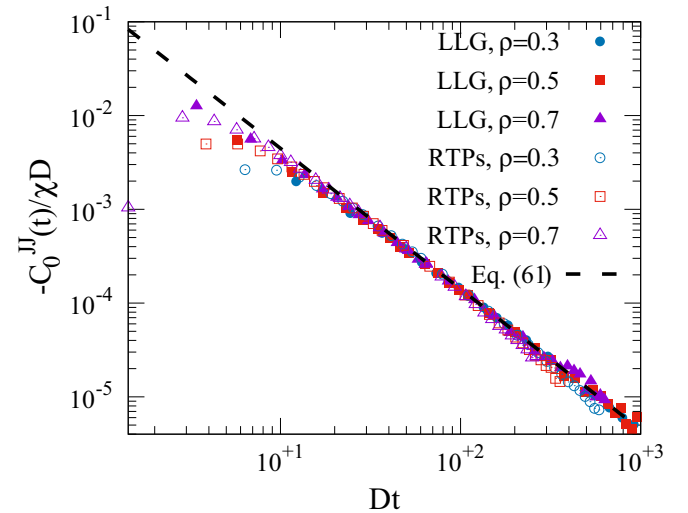

FIG. 3. Verification of Eq. (61). We plot the negative scaled equal-space unequal-time instantaneous current correlation function, i.e., $-\mathcal{C}_0^{JJ}(t)/\chi D$, as a function of Dt, for model II (LLG, closed symbols) and model I (standard RTPs, open symbols), at a fixed $\gamma = 0.1$ and different $\rho = 0.3$ (blue circle), 0.5 (red square), and 0.7 (magenta triangle). We also compare the scaled simulation data points with the theoretical prediction (black dotted line), as shown in Eq. (61).

expression for $\mathcal{C}_r^{J^{(fl)}J^{(fl)}}(t, 0)$ where $t \geqslant 0$. Using the current decomposition as in Eq. (15), we can write the following relation:

$$\mathcal{C}_r^{J^{fl}J^{fl}}(t, 0) = \mathcal{C}_r^{JJ}(t, 0) - \mathcal{C}_r^{J^DJ}(t, 0) - \mathcal{C}_r^{J^{fl}J^D}(t, 0). \quad (62)$$

Notably, the fluctuation current $J^{(fl)}(t)$ at time t is not correlated with the diffusive current $J_0^D(0)$ at an earlier time $t = 0$, i.e.,

$$\mathcal{C}_r^{J^{fl}J^D}(t, 0) = \langle J_r^{fl}(t)J_0^D(0)\rangle = 0. \quad (63)$$

Then the third term in Eq. (62) immediately drops out. Moreover, in order to determine the second term $\mathcal{C}_r^{J^DJ}(t, 0)$, we use the following relation,

$$\mathcal{C}_r^{J^DJ}(t, 0) = \left[\frac{d}{dt'}\mathcal{C}_r^{J^DQ}(t, t')\right]_{t'=0} \quad (64)$$

$$\simeq D\frac{d}{dt'}\left[\mathcal{C}_r^{\eta Q}(t, t') - \mathcal{C}_{r+1}^{\eta Q}(t, t')\right]_{t'=0}, \quad (65)$$

where we have used the truncation approximation as in Eq. (23) to arrive at Eq. (65) by using Eq. (64). Following Eq. (27), we now expand the correlators $\mathcal{C}_r^{\eta Q}(t, t')$ in the Fourier basis, and then, using Eq. (44), we obtain the desired solution,

$$\mathcal{C}_r^{J^DJ}(t, 0) = -\frac{D}{4L}\sum_q(2 - \lambda_{qr})f_q(t)e^{-\lambda_q Dt}. \quad (66)$$

Importantly the above solution coincides with the two-point unequal-time correlation of $\mathcal{C}_r^{JJ}(t, 0)$ which is displayed in the second term of Eq. (51) with $t \geqslant t' = 0$. Finally, using Eqs. (51), (63), and (66) in Eq. (62), we readily obtain

$$\mathcal{C}_r^{J^{fl}J^{fl}}(t, 0) = \langle J_r^{fl}(t)J_0^{fl}(0)\rangle = \delta(t)\Gamma_r. \quad (67)$$

E. Fluctuation of the space-time integrated current

The space-time integrated current $Q_{\text{tot}}(L, T)$ of the system is defined as

$$Q_{\text{tot}}(L, T) = \sum_{i=0}^{L-1} Q_i(T) = \int_0^T dt \sum_{i=0}^{L-1} J_i(t). \quad (68)$$

Note that $Q_{\text{tot}}(L, T)$ measures the total current in the system up to the observation time T. Alternatively, $Q_{\text{tot}}(L, T)$ can be linked to the cumulative tagged particle displacements in the following way:

$$Q_{\text{tot}}(L, T) = \sum_{i=1}^N X_i(T), \quad (69)$$

where $X_i(T)$ is the displacement of the ith particle in time T. In this section, we characterize the fluctuation properties of $Q_{\text{tot}}(L, T)$, which is essentially related to the fluctuation of cumulative displacements of RTPs in the system.

It is worth noting that, according to the decomposition shown in Eq. (15), we can write $J_i(t)$ in Eq. (68) as the sum of diffusive $J_i^{(D)}(t)$ and fluctuating $J_i^{(fl)}(t)$ current components. However, for a periodic system (which is the case here), we use the identity

$$\sum_{i=0}^{L-1} J_i^{(D)}(t) = 0, \quad (70)$$

and, as a result, the diffusive component does not contribute to $Q_{\text{tot}}(L, T)$, leading to

$$Q_{\text{tot}}(L, T) = \int_0^T dt \sum_{i=0}^{L-1} J_i^{fl}(t). \quad (71)$$

The above equation clearly reflects the fact that the time-integrated current $Q_{\text{tot}}(L, T)$ across the entire system is solely governed by the fluctuating component $J_i^{(fl)}(t)$, immediately implying the average current being zero,

$$\langle Q_{\text{tot}}(L, T)\rangle = \int_0^T dt \sum_{i=0}^{L-1} \langle J_i^{fl}(t)\rangle = 0, \quad (72)$$

since $\langle J_i^{fl}(t)\rangle = 0$. Similarly, we write the expression for the fluctuation,

$$\langle Q_{\text{tot}}^2(L, T)\rangle = \int_0^T dt' \int_0^T dt \sum_{i=0}^{L-1}\sum_r \langle J_i^{fl}(t)J_{i+r}^{fl}(t')\rangle. \quad (73)$$

Now, by using Eq. (67) in the above equation, it is straightforward to find that the total current fluctuation satisfies the following relation,

$$\frac{1}{LT}\langle Q_{\text{tot}}^2(L, T)\rangle = \sum_r \Gamma_r = 2\chi(\rho, \gamma), \quad (74)$$

where we have already expressed $\chi(\rho, \gamma)$ in terms of $P(g)$ in Eq. (48). To verify the above equation for model II (LLG), we first compute $\langle Q_{\text{tot}}^2(L, T)\rangle$ from numerical simulation with $L = 1000$ and $T = 50$ in the parameter ranges $0.01 \leqslant \rho \leqslant 0.9$ and $0.005 \leqslant \gamma \leqslant 1$. Moreover, we also numerically compute $P(g)$ and use them in Eq. (48) to obtain $\chi(\rho, \gamma)$ for the same parameter values. In Figs. 4(a) and 4(b), we plot the numerically obtained scaled fluctuation $\gamma\langle Q_{\text{tot}}^2(L, T)\rangle/2LT$ as a function of ρ and γ, respectively. We also plot the already calculated $\gamma\chi(\rho, \gamma)$ and represent them with the dotted lines. An excellent agreement between $\gamma\langle Q_{\text{tot}}^2(L, T)\rangle/2LT$ and $\gamma\chi(\rho, \gamma)$ immediately verifies Eq. (74) for model II. In Figs. 4(c) and 4(d), we plot the functional variation of the numerically obtained $\langle Q_{\text{tot}}^2(L, T)\rangle/2LT$, which is also a measure of $\chi(\rho, \gamma)$ according to Eq. (74), with respect to ρ and γ, respectively for model I (standard RTPs). Note that that the scaled fluctuation is a *nonmonotonic* function of both ρ and γ; also one can see the qualitative similarities between Figs. 4(a) and 4(c), as well as Figs. 4(b) and 4(d), thus establishing the same underlying mechanism of particle transport in models I (standard RTPs) and II (LLG).

Physically, the nonmonotonic effect in mobility in a system of interacting RTPs arises from an intricate interplay between persistence and interaction. For a fixed tumbling rate, when density increases gradually beyond the dilute regime, the number of "free" particles contributing to the current first increases, thus enhancing the particle mobility. However, this enhancement reaches a threshold density (which increases with the tumbling rate), beyond which, due to the hardcore
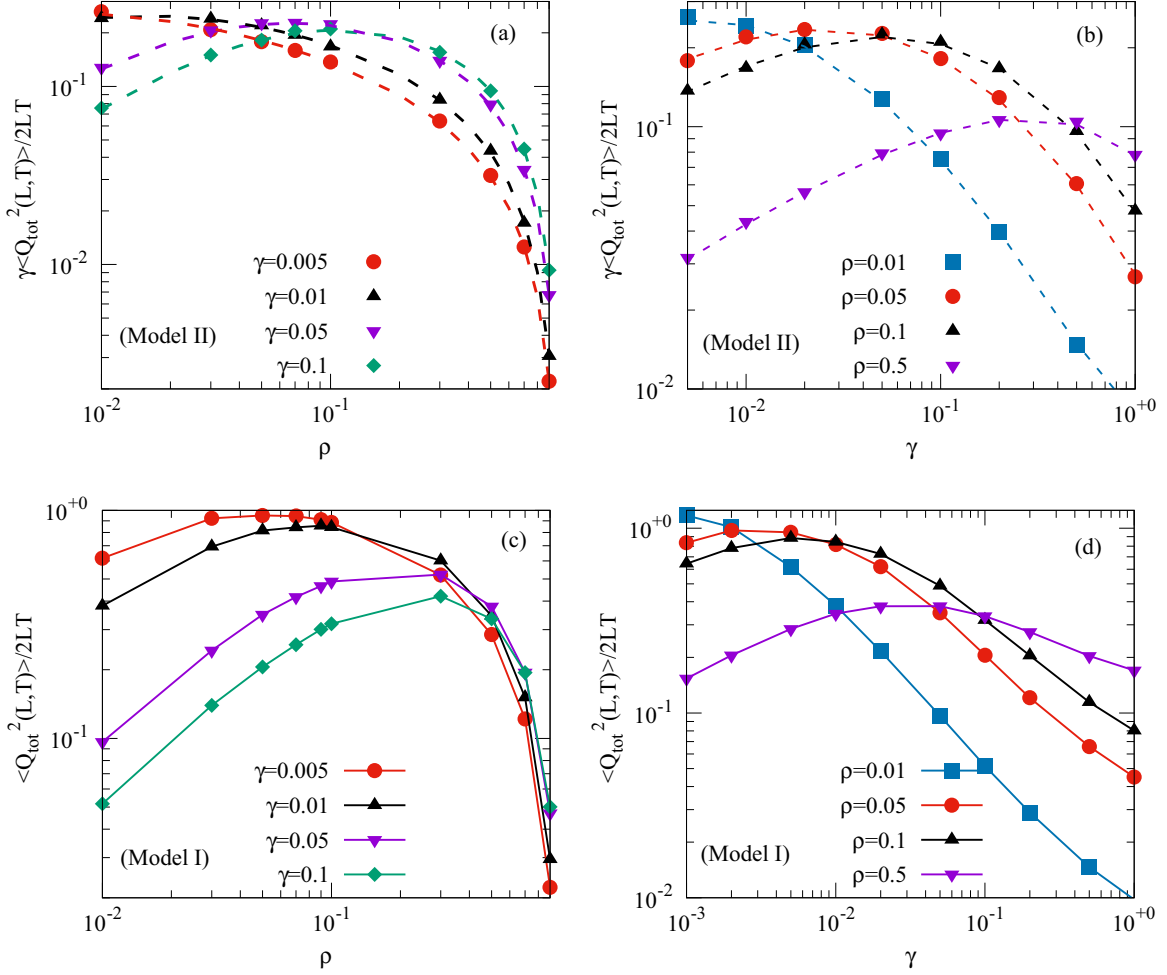
FIG. 4. [(a) and (b)] Scaled space-time integrated current fluctuation $\gamma \langle Q_{tot}^2(L, T) \rangle / 2LT$ for the LLG, obtained from simulation (points), as a function of ρ [at different $\gamma = 0.001$ (blue square), 0.005 (red circle), 0.01 (black triangle), 0.05 (magenta inverted triangle), and 0.1 (green diamond)] and γ [at various $\rho = 0.01$ (blue square), 0.05 (red circle), 0.1 (black triangle), and 0.5 (magenta inverted triangle)], respectively. Corresponding dotted lines are $\gamma \chi(\rho, \gamma)$ calculated by using the numerically obtained $P(g)$ in Eq. (48). The excellent match between these two quantities verifies Eq. (74). [(c) and (d)] Plots of $\langle Q_{tot}^2(L, T) \rangle / 2LT$ for model I (standard RTPs), obtained from numerical simulation (line point), as a function of ρ and γ, respectively, for the aforementioned parameters.

interaction, particles form clustered (thus almost immobile) configurations, reducing the number of "free" RTPs and hence resulting in the decrease in mobility. This explains the above-mentioned nonmonotonicity as seen from Figs. 4(a) and 4(c). Likewise, as seen in Figs. 4(b) and 4(d), for a fixed density, decreasing γ amplifies the persistence effect, thus increasing the total current fluctuation and therefore also the mobility. Further reduction in γ corresponds to very large persistence, facilitating clustered (almost immobile) configurations, that decrease the particle mobility. Notably, between these extremes, there must exists a threshold γ (which increases with ρ), where the competing effects of persistence and interaction result in an optimal transport in the system.

Scaling regime for the particle mobility $\chi(\rho, \gamma)$

In this section, we study the particle mobility $\chi(\rho, \gamma)$ in the two limiting cases: case I, $\rho \to 0$, $\gamma \to \infty$, and case II, $\rho \to 0$, $\gamma \to 0$. While case I is qualitatively similar to the SSEP limit, case II captures the nontrivial interplay of

interaction and persistence in terms of the scaling variable $\psi = \rho/\gamma$. Previously, in Ref. [14], we investigated a similar scaling regime for the bulk-diffusion coefficient $D(\rho, \gamma)$ for case II; also, in the case of the mobility, we calculate the associated scaling function analytically for model II, by using the truncation scheme as in Eq. (23).

By using Eqs. (53) and (48), we substitute the steady-state gap distribution $P(g)$ in $\chi(\rho, \gamma)$ for model II and obtain

$$\chi(\rho, \gamma) \simeq \frac{(1 - \rho)}{2} \frac{(e^{1/g_*} - 1)(e^{\gamma + 1/g_*} + 1)}{(e^{\gamma + 1/g_*} - 1)^2}. \tag{75}$$

Note that the above expression of $\chi(\rho, \gamma)$ is valid for any arbitrary ρ and γ. However, in the following discussion, we analyze the limiting cases mentioned in the beginning.

Case I ($\rho \to 0$ and $\gamma \to \infty$). In this case of small persistence and low-density limit, the steady-state distribution is a product measure: $P(g) \sim (1 - \rho)^g \simeq e^{-\rho g}$, yielding $g_* = 1/\rho$. Finally, using this g_* and setting the condition $\gamma \gg 1 \gg$

ρ in Eq. (75), we obtain

$$\chi(\rho, \gamma) \simeq \frac{e^{-\gamma}}{2}\rho(1-\rho) = \frac{e^{-\gamma}}{2}\chi^{(0)}, \qquad (76)$$

which, up to a scale factor $\exp(-\gamma)$ due to time scaling (explained below), is the particle mobility $\chi^{(0)} = \rho(1-\rho)$ in SSEP. The exponential prefactor $e^{-\gamma}$ in the above equation appears because of the following. In this case, $\phi(l)$ carries maximum weight at $l = 0$, while all other hop lengths, i.e., $l > 0$, occur with an exponentially smaller probability $1 - \phi(0) = e^{-\gamma}$. Furthermore, among these nonzero hop lengths, $l = 1$ dominates, with contributions from the larger l being vanishingly small. Therefore, in the limit $\gamma \to \infty$ or, equivalently, $l_p \to 0$ in model II (LLG), particles effectively perform SSEP-like hopping dynamics, albeit with a rate that is simply exponentially small, $e^{-\gamma}$, thus explaining the prefactor in Eq. (76).

Case II ($\rho \to 0$ and $\gamma \to 0$). As we show below, similar to the bulk-diffusion coefficient $D(\rho, \gamma)$ in hardcore RTPs studied in Ref. [14], the particle mobility too exhibits interesting scaling properties. Indeed, in the strong-persistence and low-density limits, there are only two relevant length scales in the problem: the persistence length $l_p = v/\gamma$ and the "mean free path" or the average gap $\langle g \rangle \simeq 1/\rho$. Consequently, their ratio $\psi = l_p/\langle g \rangle$ is expected to provide a scaling variable that should quantify the interplay of persistence and interaction. In the regime of strong persistence, $\psi \to \infty$ denotes the strongly interacting limit, whereas $\psi \to 0$ corresponds to the noninteracting limit. Now, as argued previously in Ref. [14], we have the typical gap length g_* satisfying the following scaling law: $g_* \simeq \mathcal{G}(\psi)/\rho$. In the limit of $\psi \to 0$, the model reduces to the well-known SSEP for which $\mathcal{G}(\psi) = 1$, while, in the opposite limit of $\psi \to \infty$, we have the strongly interacting regime, for which previous calculations in Ref. [49] yield $\mathcal{G}(\psi) = \sqrt{\psi}$. Now combining these two limiting cases, we could simply write $\mathcal{G}(\psi) \simeq \sqrt{1 + \psi}$. Finally, plugging the assumed form of $g_* = \mathcal{G}(\psi)/\rho$ in Eq. (75), and after some algebraic manipulations, we obtain the following scaling law:

$$\chi_{\text{LLG}}(\rho, \gamma) \equiv \frac{\chi^{(0)}}{\gamma^2}\mathcal{H}_{\text{LLG}}\left(\psi = \frac{\rho}{\gamma}\right), \qquad (77)$$

where $\chi^{(0)} = \rho(1-\rho)$ is the particle mobility in the SSEP and the expression for the scaling function can be explicitly written as

$$\mathcal{H}_{\text{LLG}}(\psi) = \frac{\mathcal{G}(\psi)}{(\psi + \mathcal{G}(\psi))^2}. \qquad (78)$$

Finally for model II (LLG), by replacing the above form of $\mathcal{G}(\psi) \simeq \sqrt{1 + \psi}$, we immediately obtain

$$\mathcal{H}_{\text{LLG}}(\psi) = \frac{\sqrt{1+\psi}}{(\psi + \sqrt{1+\psi})^2} \qquad (79)$$

(for calculation details, see Appendix I).

In the top panel of Fig. 5, we plot the scaled mobility $\gamma^2\chi_{\text{LLG}}(\rho, \gamma)/\chi^{(0)}$, obtained from simulations (points), as a function of the scaling variable $\psi = \rho/\gamma$ in the parameter ranges $0.01 \leqslant \rho \leqslant 0.5$ and $0.001 \leqslant \gamma \leqslant 0.1$. We observe that the data points collapse onto each other and that the collapsed data points follow the analytically obtained scaling function $\mathcal{H}_{\text{LLG}}(\psi)$ (solid line) quite well. This observation
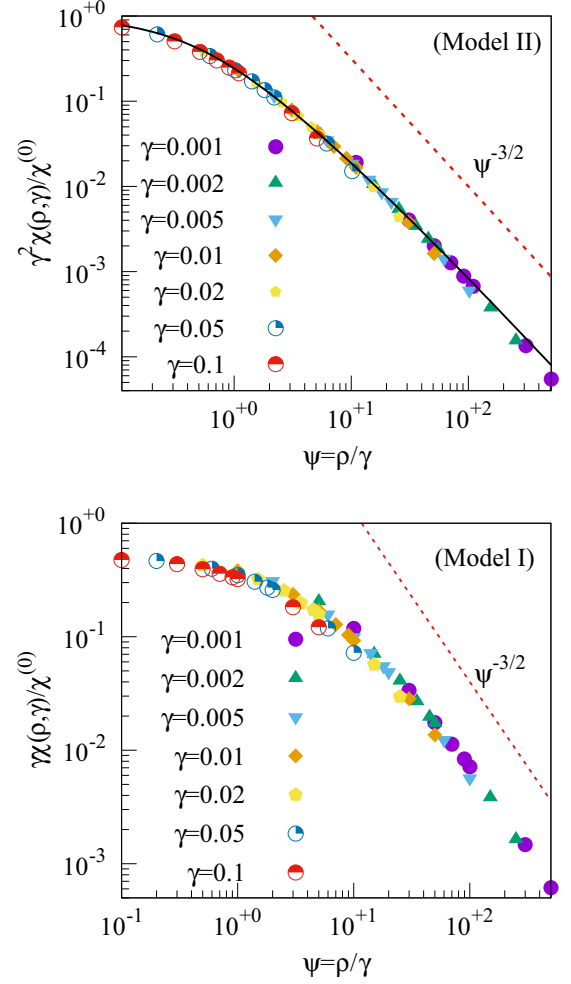

FIG. 5. Verification of Eqs. (77) and (79). We plot the ratio $\gamma^a\chi(\rho, \gamma)/\chi^{(0)}$ for model II (LLG, top panel, $a = 2$) and model I (RTPs, bottom panel, $a = 1$) as a function of scaling variable $\psi = \rho/\gamma$ in the parameter ranges $0.01 \leqslant \rho \leqslant 0.5$ and $0.001 \leqslant \gamma \leqslant 0.1$. For LLG, we compare the collapsed simulation data points with the analytic scaling function $\mathcal{H}_{\text{LLG}}(\psi)$ (solid black line) shown in Eq. (79). For both models, the collapsed data points exhibit $\psi^{-3/2}$ decay in the asymptotic limit, which is shown here by the red dotted line.

indeed verifies the existence of the scaling law as in Eq. (77) and substantiates the scaling function derived in Eq. (79). We find that the same scaling law holds also for model I (standard RTPs). To demonstrate this, we plot $\gamma\chi_{RTP}(\rho, \gamma)/\chi^{(0)}$ as a function of ψ in the bottom panel of Fig. 5, in the same parameter range as in LLG.

F. Time-integrated bond-current fluctuation

To calculate the steady-state time-integrated bond-current fluctuation, we simply put $r = 0$ and $t' = t = T$ in Eq. (49) and obtain

$$\mathcal{C}_0^{QQ}(T, T) = \Gamma_0 T - \frac{1}{L}\sum_q \frac{f_q}{\lambda_q}\left\{t - \frac{(1 - e^{-\lambda_q DT})}{\lambda_q D}\right\} \qquad (80)$$

$$= \frac{2\chi}{L}T + \frac{1}{DL}\sum_q \frac{f_q}{\lambda_q^2}(1 - e^{-\lambda_q DT}) \qquad (81)$$

[see Appendix G for the derivation of Eq. (81)]. It is important to mention that $\mathcal{C}_0^{QQ}(T, T)$, which is expressed by Eqs. (80) and (81) in its most comprehensive form, exhibits quite interesting characteristics at different time regimes. In the subsequent discussion, we investigate these properties by analyzing the limiting cases.

1. Case I: Small-time regime $DT \ll 1$

In this case, we perform a linear expansion of the exponential function in the second term of Eq. (80) with respect to DT, which yields $e^{-\lambda_q DT} \approx 1 - \lambda_q DT$. As a result, this term drops out and we are left with

$$\mathcal{C}_0^{QQ}(T, T) \simeq \Gamma_0 T, \tag{82}$$

where Γ_0 is simply obtained by putting $r = 0$ in Eq. (46).

2. Case II: Intermediate- and long-time regime $DT \gg 1$

In general, it is difficult to evaluate the summation in the second term of Eq. (81) in a closed form. However, in this time regime, the summand only contributes when $q \to 0$ and vanishes otherwise. In this limit, the eigenvalues are quadratic, i.e., $\lambda_q \simeq q^2$, $\lambda_{gq} \simeq g^2 q^2$, and $\lambda_{lq} \simeq l^2 q^2$, resulting in a simplified version of Eq. (81),

$$\mathcal{C}_0^{QQ}(T, T) \simeq \frac{2\chi}{L} \left[T + \frac{1}{D} \sum_q \frac{1}{\lambda_q^2} (1 - e^{-\lambda_q DT}) \right]. \tag{83}$$

Considering both of the preceding cases, the asymptotic behavior of $\mathcal{C}_0^{QQ}(T, T) = \langle Q^2(t) \rangle$ is obtained as

$$\langle Q^2(T) \rangle \simeq \begin{cases} \Gamma_0 T & \text{for } DT \ll 1 \\ \frac{2\chi(\rho, \gamma)}{\sqrt{\pi D(\rho, \gamma)}} \sqrt{T} & \text{for } 1 \ll DT \ll L^2 \\ \frac{2\chi(\rho, \gamma)}{L} T & \text{for } DT \gg L^2, \end{cases} \tag{84}$$

where the first term simply corresponds to Eq. (82), while the other two terms are obtained using Eq. (83) (for details, see Appendix H). Therefore, the time-integrated bond-current fluctuation $\langle Q_i^2(T) \rangle$ exhibits an initial linear growth in time before transitioning to a subdiffusive scaling at the intermediate regime $L^2/D \gg T \gg 1/D$; subsequently, at larger timescales $T \gg L^2/D$, it reverts to diffusive or linear scaling behavior where the strength of the fluctuation is governed by $\chi(\rho, \gamma)$. To verify these observations, we plot the numerically obtained bond-current fluctuation $\langle Q_i^2(T) \rangle$ as a function of the observation time T, at the top panel of Fig. 6 for LLG at different parameter values and compare them with our analytical solution given in Eq. (81). Note that we have calculated the bulk-diffusion coefficient $D(\rho, \gamma)$, which appears in Eq. (81), by numerically calculating the steady-state gap distribution function $P(g)$ and then by using the exact analytic expression given in Eq. (14). We find that the numerical data points clearly exhibit the previously mentioned three different regimes and they follow the analytical solution quite well. In the case of model I (standard RTPs), we plot the similar quantity, obtained from direct simulations, in the bottom panel of Fig. 6. We find that, in the above-mentioned time regimes, the data points have quite similar characteristics as in model II (LLG).
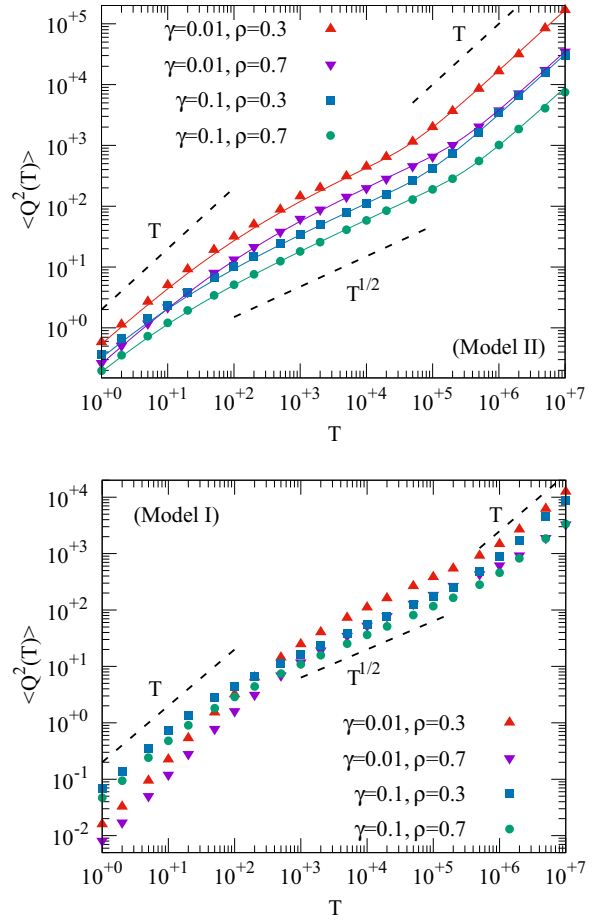

FIG. 6. We plot the time-integrated bond-current fluctuation $\langle Q_i^2(T) \rangle$, as a function of time T, obtained from simulations (points) for model II (LLG, top panel) and model I (standard RTPs, bottom panel) at $\rho = 0.3, 0.7$ and $\gamma = 0.1, 0.01$. In the case of model II, we also compare the simulation data points with the analytical solution shown in Eq. (81) (line). For both these models, $\langle Q_i^2(T) \rangle$ exhibits subdiffusive growth at the intermediate-time regime, followed by a diffusive (linear) growth at very long times (shown by the dotted lines).

Interestingly, the above intermediate- and long-time regime for time-dependent bond-current fluctuations can actually be unified through a single scaling function as follows. Moreover, quite remarkably, the scaling function seems to be universal, as it does not depend on the details of the dynamical rules of the models considered here. In the limit of $L \to \infty$ and $DT \to \infty$ such that $y = DT/L^2$ is finite, we find $\mathcal{C}_0^{QQ}(T, T) = \langle Q^2(T) \rangle$, as expressed in Eq. (83), to satisfy the following scaling relation:

$$\frac{D}{2\chi L} \langle Q^2(T) \rangle = \mathcal{W}\left(\frac{DT}{L^2} \right). \tag{85}$$

For model II (LLG), the scaling function is calculated exactly within the truncation scheme and is given by the following series:

$$\mathcal{W}(y) = y + \lim_{L \to \infty} \frac{1}{L^2} \sum_q \frac{1}{\lambda_q} (1 - e^{-\lambda_q y L^2}). \tag{86}$$
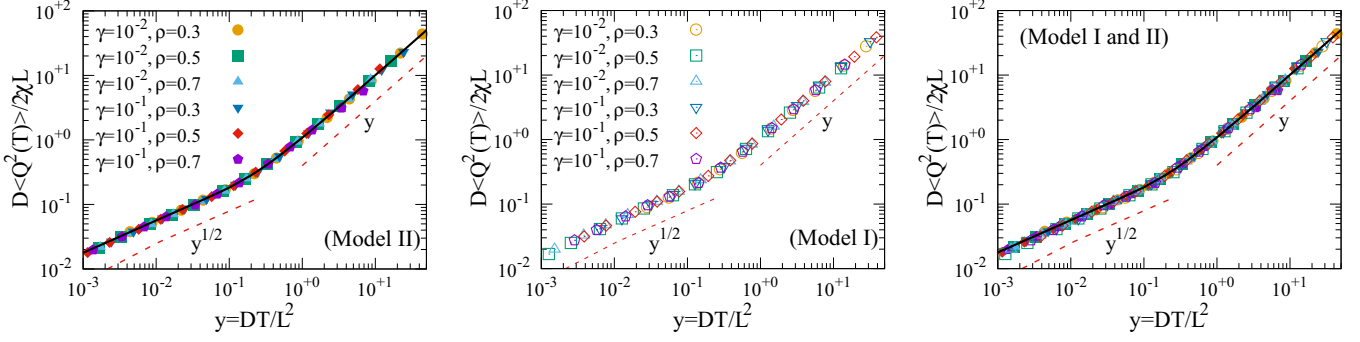
FIG. 7. Verification of Eqs. (85) and (86). We plot the scaled bond-current fluctuation $D\langle Q_i^2(T)\rangle/2\chi L$ for model II (LLG, left-hand panel) and model I (standard RTPs, middle panel), obtained from simulations (points) at various ρ and γ, as a function of the rescaled hydrodynamic time $y = D(\rho, \gamma)T/L^2$. For LLG, we compare the scaled data points with the analytic scaling function $\mathcal{W}(y)$ shown in Eq. (86) (black line). In the right-hand panel, we check the universality of $\mathcal{W}(y)$ by plotting these numerically obtained scaled current fluctuation $D\langle Q_i^2(T)\rangle/2\chi L$ for model II (LLG, closed points) and model I (standard RTPs, open points) together and compare them with the analytically obtained $\mathcal{W}(y)$. In all three panels, the red dotted guiding lines reflect the early time subdiffusive growth ($\sim \sqrt{y}$), followed by the diffusive growth of $\mathcal{W}(y) \sim y$ as derived in Eq. (88).

One can approximate the discrete sum in the right-hand side of the above equation as a quadrature, which can be written as [51]

$$\mathcal{W}(y) \simeq y + \left(\frac{y}{\pi}\right)^{1/2} \text{erfc}(2\pi\sqrt{y}) + \frac{1 - \exp(-4\pi^2 y)}{4\pi^2},$$
(87)

with $\text{erfc}(y) = 1 - \text{erf}(y)$ and the error function $\text{erf}(y) = (2/\sqrt{\pi})\int_0^y \exp(-t^2)dt$. Note that, as demonstrated in Fig. 7, the scaling function is the same for both models I and II. We also perform an asymptotic analysis to obtain the behavior of $\mathcal{W}(y)$ in the two limiting cases when $y \ll 1$ and $y \gg 1$ and we find the following:

$$\mathcal{W}(y) \simeq \begin{cases} \sqrt{y/\pi} & \text{for } y \ll 1 \\ y & \text{for } y \gg 1. \end{cases}$$
(88)

To verify our theoretical results, as in Eqs. (83), (86), and (88), we plot in Fig. 7 the steady-state scaled bond-current fluctuations as a function of the rescaled hydrodynamic time $y = DT/L^2$ for models II (LLG, left-hand panel) and I (standard RTPs, right-hand panel) for various ρ and γ denoted; simulation results are represented the points. We determine $D(\rho, \gamma)$ and $\chi(\rho, \gamma)$ for model II (LLG) by numerically evaluating $P(g)$ in the steady state and utilizing it in Eqs. (14) and (48), respectively. In contrast, for model I (standard RTPs), we compute $D(\rho, \gamma)$ by studying the relaxation of a long-wavelength perturbation, following the approach outlined in our previous work [14], and for the mobility $\chi(\rho, \gamma)$, we calculate the scaled space-time integrated current fluctuation using the formula provided in Eq. (74). For both models, we see an excellent collapse of the simulation data points. The collapsed data (points) follow the analytically derived scaling function $\mathcal{W}(y)$ as given in Eq. (86) (line) and they exhibit subdiffusive growth at small y before crossing over to diffusive growth at large y, thus being consistent with the asymptotic form as in Eq. (88).

IV. SUMMARY AND CONCLUDING REMARKS

In this work, we characterize steady-state current fluctuations in two minimal models of athermal hardcore RTPs by using a microscopic approach. Model I is the standard version of hardcore RTPs introduced in Ref. [47], whereas model II is a long-ranged lattice gas (LLG)—a variant of model I [14]; the latter model also has the hardcore constraint. These two model systems were recently considered by us in Ref. [14], where we characterized the collective- or bulk-diffusion coefficient; in this study, we characterize the other transport coefficient, the collective particle mobility, which essentially characterizes current fluctuations in the system. Indeed, one great advantage of studying model II (LLG) is that, despite a lack of knowledge of the steady-state measure having nontrivial spatial correlations, the model is amenable to analytical studies and is the primary focus of our work. To this end, we introduce a truncation (closure) scheme in our microscopic dynamical framework to analytically calculate various dynamic quantities, which have been of significant interest in the past in the context of self-propelled particles. In particular, in model II, we calculate exactly, within the truncation approximation, the fluctuations of time-integrated current $Q_i(T)$ across a bond $(i, i + 1)$ in a time interval T as well as instantaneous current $J_i(t) \equiv dQ_i(t)/dt$. We compare our theoretical results with those obtained from direct Monte Carlo simulations of models I and II and observe that the two models of RTPs share remarkably similar features.

The main results of this paper are as follows. The time-integrated bond-current fluctuation exhibits subdiffusive growth at moderately large time $r_0^2/D \ll T \ll L^2/D$ (with r_0 being the lattice spacing, or particle diameter, taken to be unity throughout), where $\langle Q_i(T)^2\rangle \sim T^{1/2}$, before crossing over to a diffusive growth regime at very long time $T \gg L^2/D$, where $D(\rho, \gamma)$ is the density- and tumbling-rate-dependent bulk-diffusion coefficient [14]. Notably, the power-law behaviors are qualitatively similar to those observed in symmetric exclusion processes [33]. Although the prefactors in the growth laws as a function of density and tumbling rate are

model dependent, they can be expressed in terms of the two macroscopic transport coefficients: the bulk-diffusion coefficient and the mobility. Remarkably, in the limit of L, T being large, with the dimensionless scaling variable DT/L^2 finite, we show that the growth of time-integrated bond-current fluctuation obeys a scaling law, that is presumably universal, i.e., independent of the dynamical rules of the models and parameter values [see Eq. (85)].

Furthermore, using the truncation scheme introduced in our microscopic theory, we analytically calculate in model II (LLG) the fluctuations of space-time integrated current across the entire system (equivalently, the cumulative displacement of all particles). In this way, we can characterize the current fluctuations in terms of the collective particle mobility $\chi(\rho, \gamma) \equiv \lim_{L \to \infty} (1/2LT) \langle [\sum_{i=1}^{L} Q_i^2(T)] \rangle_c$ [see Eq. (74)], which is also equal to the scaled space-time integrated fluctuating ("noise") current. Interestingly, in the limit of small density and strong persistence, i.e., $\rho, \gamma \to 0$ with scaling variable $\psi = \rho/\gamma \sim l_p/\bar{g}$ fixed, we show that, similar to the bulk-diffusion coefficient $D(\rho, \gamma)$ studied in Ref. [14], there exists a scaling regime for the mobility $\chi(\rho, \gamma)$ too. Indeed, the scaling regime implies that the system is governed by essentially only *two* length scales: the persistence length $l_p \sim \gamma^{-1}$ and the mean gap $\bar{g} \sim 1/\rho$ [14]. Thus, our analysis highlights the crucial role of persistence and interaction in the collective relaxation and fluctuation in the conventional models of hardcore RTPs.

Moreover, our theoretical scheme readily allows us to calculate the spatial and dynamic properties of the instantaneous current in model II (LLG). Using our microscopic calculations, we derive that, at long times, the two-point dynamic correlation function for instantaneous bond-current as a function of time t is indeed a power law of the form $\sim t^{-3/2}$ and, moreover, it is negative for $t \neq 0$, with a delta-correlated part at the origin $t = 0$. Similar behavior is also observed for model I (standard hardcore RTPs). On the other hand, the spatial correlations of current in both models are found to decay exponentially, $\exp(-r/\xi)$, with spatial separation r. Interestingly, in the strong-persistence regime, we find that correlation length ξ *diverges* as the square root of persistence time τ_p, i.e., $\xi \sim \sqrt{\tau_p}$, the behavior which we derive analytically for model II (LLG). This result provides a microscopic theoretical explanation of the qualitative features of velocity correlations observed in the recent experiments and simulations [21,27].

Characterizing current fluctuations in driven many-body systems having a nontrivial spatial structure is a difficult problem in general and exact calculations of the dynamic current correlations have been done for few such systems so far [51]. Previously, an exact calculation of the temporal growth of the time-integrated bond current has been performed for the symmetric simple exclusion process (SSEP), which, despite having hardcore interactions, however, has a product measure and, as a result, does not have spatial correlations [33]. However, the above analysis for the SSEP cannot be easily extended to systems with finite spatial correlations, which is the case here. This is because, in such a case, the equations governing the two-point correlations involve higher-order correlations, resulting in an infinite hierarchy of many-body correlations. To get around the difficulty, in this paper we use a truncation scheme [16], which, though approximate, immediately leads to a closed set of equations for density and current correlations, thus making model II (LLG) analytically tractable.

Indeed, deriving a rigorous fluctuating hydrodynamics for interacting SPPs is a fundamental problem in nonequilibrium statistical physics and our present work provides some useful insights in that direction. Previously, some progress has been made in Ref. [43], albeit only for a special class of "weakly interacting" RTPs (with vanishing spatial correlations in the thermodynamic limit), where tumbling rate and velocity are system-size dependent and vanishingly small. In that case, the system has two slowly varying fields, density and "magnetization," which are in fact coupled on hydrodynamic scales. However, as discussed below, in our present work we consider the conventional RTPs having finite, system-size independent, tumbling rates (which could be small though). The findings of this study, along with our previous study of density relaxation in hardcore RTPs in Ref. [14], implies that, for finite tumbling rates, one can, on timescales much larger than the persistence time, integrate out the magnetization field. Then the resulting large-scale fluctuating hydrodynamics will be effectively governed by Eq. (1); the crucial ingredients of this theory are the macroscopic density- and tumbling-rate-dependent bulk-diffusion coefficient [14] and mobility, which we characterize here.

It is worth noting that the order of limits, tumbling rate $\gamma \to 0$, and system size $L \to \infty$, is important, and, depending on the order, there can be various distinct circumstances as described below.

(1) As one takes the limit $\gamma \to 0$ first and then the limit $L \to \infty$ (by keeping drift velocity v fixed), the system eventually goes into a state of *dynamical arrest* [52], where dynamical activities cease and the system becomes frozen in time.

(2) The tumbling rate $\gamma(L) \sim \mathcal{O}(L^{-\delta_1})$ and drift velocity $v(L) \sim \mathcal{O}(L^{-\delta_2})$ are taken to be system-size dependent and one takes the limit $L \to \infty$, by keeping diffusion rate fixed; a specific case with $\delta_1 = 2$ and $\delta_2 = 1$ was considered in Refs. [42] and [44].

(3) On the other hand, in the present work, we consider conventional (athermal) hardcore RTPs (therefore, "strongly interacting") in the limit of L large, with γ fixed (thermal or bare diffusion rate is strictly zero) [14]. We are particularly interested in the $\gamma \to 0$ limit, but, in that case, the $L \to \infty$ limit is taken first; in other words, persistent length $l_p = v/\gamma$ is finite and large, but much smaller than the system size L, $1 \ll l_p \ll L$. We keep the drift velocity v fixed.

Notably, our theory is based on two important assertions [10,19]: (i) the total instantaneous current can be decomposed into a diffusive and a fluctuating ("noise") component, with the latter having mean zero and short-ranged (in fact, delta-correlated for model II) temporal correlations, and (ii) the diffusive current can be written as a product of the bulk-diffusion coefficient and the gradient of mass (occupation) variable. The latter implies that the local relaxation processes are effectively "slaved" to coarse-grained local density, implying a "local-equilibrium-like" property of the steady state and thus diffusive relaxation on long timescales. Indeed, our theory leads to the explicit analytical calculation of various

quantities, such as current fluctuations, mobility [see Eqs. (81) and (48)], and scaling properties [see Eqs. (85) and (77)]—all of which agree remarkably well with simulations (see Figs. 7 and 5). Furthermore, the comparison of models I and II shows that the two systems have qualitatively similar spatiotemporal behaviors. The striking resemblance suggests that the typical models of interacting RTPs can be described by the same theoretical framework, formulated in terms of the two macroscopic transport coefficients: the bulk-diffusion coefficient and the collective particle mobility. Indeed, dynamic fluctuations in interacting SPPs have not yet been fully understood and, unlike the linear-response theory for equilibrium systems, a general theoretical formulation for dealing with such systems is still lacking. In this scenario, our study elucidates the large-scale hydrodynamic structure of hardcore RTPs and could initiate further studies concerning interacting SPPs in general.

APPENDIX A: TIME EVOLUTION OF TWO-POINT UNEQUAL-TIME CURRENT-CURRENT CORRELATION $\mathcal{C}_r^{QQ}(t', t)$

$$
Q_r(t' + dt')Q_0(t) = \begin{cases} (Q_r(t') + 1)Q_0(t), & \text{prob.} \quad \mathcal{P}_r^R dt' \\ (Q_r(t') - 1)Q_0(t), & \text{prob.} \quad \mathcal{P}_r^L dt' \\ Q_r(t')Q_0(t), & \text{prob.} \quad 1 - \left(\mathcal{P}_r^R + \mathcal{P}_r^L\right)dt'. \end{cases} \tag{A1}
$$

Using the update rules in Eq. (A1) and substituting the expressions of $\mathcal{P}_r^R$ and $\mathcal{P}_r^L$, as shown in Eqs. (7) and (8), respectively, the corresponding time-evolution equation can be written as

$$
\frac{d}{dt'}\langle Q_r(t')Q_0(t)\rangle = \frac{1}{2}\sum_{l=1}^{\infty}\phi(l)\left[\left\{\langle\hat{\mathcal{U}}_{r+l}^{(l)}(t')Q_0(t)\rangle - \langle\hat{\mathcal{U}}_r^{(l)}(t')Q_0(t)\rangle\right\} + \sum_{g=1}^{l-1}\left\{\langle\hat{\mathcal{V}}_{r+g+1}^{(g+2)}(t')Q_0(t)\rangle - \langle\hat{\mathcal{V}}_{r+1}^{(g+2)}(t')Q_0(t)\rangle\right\}\right]. \tag{A2}
$$

Finally, using the definition of $\mathcal{C}_r^{QQ}(t', t)$ as provided in Eq. (18), we immediately obtain

$$
\frac{d}{dt'}\mathcal{C}_r^{QQ}(t', t) = \frac{1}{2}\sum_{l=1}^{\infty}\phi(l)\left[\left\{\mathcal{C}_{r+l}^{\mathcal{U}^{(l)}Q}(t', t) - \mathcal{C}_r^{\mathcal{U}^{(l)}Q}(t', t)\right\} + \sum_{g=1}^{l-1}\left\{\mathcal{C}_{r+g+1}^{\mathcal{V}^{(g+2)}Q}(t', t) - \mathcal{C}_{r+1}^{\mathcal{V}^{(g+2)}Q}(t', t)\right\}\right] \tag{A3}
$$

$$
= \left\langle J_r^{(D)}(t')Q_0(t)\right\rangle_c. \tag{A4}
$$

Here we have used the expression for $J_r^{(D)}(t')$ as given in Eq. (16). Note that the above two equations are expressed in the main text as Eqs. (19) and (20).

APPENDIX B: TIME EVOLUTION OF THE TWO-POINT UNEQUAL-TIME DENSITY-CURRENT CORRELATION $\mathcal{C}_r^{\eta Q}(t', t)$

In this section, we derive the time-evolution equation for the two-point unequal-time density-current correlation $\mathcal{C}_r^{\eta Q}(t', t)$ as shown in Eq. (26) in the main text. In order to do so, we first derive the time-evolution equation of the local density $\rho_r(t)$, which is defined as the average occupancy at site r and time t, i.e., $\rho_r(t) = \langle\eta_r(t)\rangle$.

Recall that the average instantaneous bond current $\langle J_r(t)\rangle$ across the bond $(r, r+1)$ at time t [as given by Eq. (9) in the main text] is given by

$$
\langle J_r(t)\rangle = \frac{1}{2}\sum_{l=1}^{\infty}\phi(l)\left[\sum_{g=1}^{l-1}\left(\mathcal{V}_{r+g+1}^{(g+2)} - \mathcal{V}_{r+1}^{(g+2)}\right) + \left(\mathcal{U}_{r+l}^{(l)} - \mathcal{U}_r^{(l)}\right)\right]. \tag{B1}
$$

Since the total number of particles is a conserved quantity, the corresponding local density is a slow variable, and its time evolution must be related to $\langle J_r(t)\rangle$ via the following continuity equation:

$$
\frac{d\rho_r(t)}{dt} = \langle J_{r-1}(t)\rangle - \langle J_r(t)\rangle. \tag{B2}
$$

Using Eq. (B1) in Eq. (B2), it is now straightforward to obtain the corresponding time-evolution equation in the form of the following balance equation:

$$\frac{d\rho_r(t)}{dt} = \langle \mathcal{P}_r^+(t) \rangle - \langle \mathcal{P}_r^-(t) \rangle, \tag{B3}$$

where the gain and loss terms are respectively given by

$$\mathcal{P}_r^+(t) = \frac{1}{2} \sum_{l=1}^{\infty} \phi(l) \left[\sum_{g=1}^{l-1} \left\{ \mathcal{V}_{r+g}^{(g+2)} + \mathcal{V}_{r+1}^{(g+2)} \right\} + \left\{ \left(\mathcal{U}_{r+l-1}^{(l)} - \mathcal{U}_{r+l}^{(l+1)} \right) + \left(\mathcal{U}_r^{(l)} - \mathcal{U}_r^{(l+1)} \right) \right\} \right], \tag{B4}$$

$$\mathcal{P}_r^-(t) = \frac{1}{2} \sum_{l=1}^{\infty} \phi(l) \left[\sum_{g=1}^{l-1} \left\{ \mathcal{V}_{r+g+1}^{(g+2)} + \mathcal{V}_r^{(g+2)} \right\} + \left\{ \left(\mathcal{U}_{r+l}^{(l)} - \mathcal{U}_{r+l}^{(l+1)} \right) + \left(\mathcal{U}_{r-1}^{(l)} - \mathcal{U}_{r+l}^{(l+1)} \right) \right\} \right]. \tag{B5}$$

We now use the expression of the local diffusive current operator, as shown in Eq. (16) in the main text, to arrive at the following identity:

$$\mathcal{P}_r^+(t) - \mathcal{P}_r^-(t) = J_{r-1}^{(D)}(t) - J_r^{(D)}(t) \tag{B6}$$

$$\simeq D(\rho, \gamma)[\eta_{r+1}(t) + \eta_{r-1}(t) - 2\eta_r(t)], \tag{B7}$$

where Eq. (B7) is a direct consequence of the proposed closure approximation, as shown in Eq. (23) in the main text. Finally, using Eqs. (B7) and (B3) together, we arrive at the desired time-evolution equation,

$$\frac{d\rho_r(t)}{dt} \simeq D(\rho, \gamma)[\rho_{r+1}(t) + \rho_{r-1}(t) - 2\rho_r(t)] = D(\rho, \gamma)\Delta_r^2 \rho_r(t), \tag{B8}$$

where Δ_r^2 is the discrete Laplacian operator. We will now deduce the desired time evolution of $\mathcal{C}_r^{\eta Q}(t', t)$ by writing the following update rules:

$$\eta_r(t' + dt')Q_0(t) = \begin{cases} 1 \times Q_0(t), & \text{prob.} \quad \mathcal{P}_r^+(t')dt' \\ 0 \times Q_0(t), & \text{prob.} \quad \mathcal{P}_r^-(t')dt' \\ \eta_r(t)Q_0(t), & \text{prob.} \quad 1 - \Sigma dt. \end{cases} \tag{B9}$$

Using the update equation, as shown above in Eq. (B9), we write down the corresponding time-evolution equation as

$$\frac{d}{dt'} \langle \eta_r(t')Q_0(t) \rangle = \langle (\mathcal{P}_r^+(t') - \mathcal{P}_r^-(t'))Q_0(t) \rangle \tag{B10}$$

$$\simeq D(\rho, \gamma)\Delta_r^2 \langle \eta_r(t')Q_0(t) \rangle, \tag{B11}$$

where in the last equation, we have used the identity displayed in Eq. (B7). Now, by using the definition of $\mathcal{C}_r^{\eta Q}(t', t) = \langle \eta_r(t')Q_0(t) \rangle - \langle \eta_r(t') \rangle Q_0(t) \rangle$, we directly obtain

$$\frac{d}{dt'} \mathcal{C}_r^{\eta Q}(t', t) \simeq D(\rho, \gamma)\Delta_r^2 \mathcal{C}_r^{\eta Q}(t', t). \tag{B12}$$

Note that Eq. (B12) is the desired time-evolution equation which we have used in Eq. (26) in the main text.

APPENDIX C: TIME EVOLUTION OF THE EQUAL-TIME DENSITY-CURRENT CORRELATION $\mathcal{C}_r^{\eta Q}(t, t)$

Here we will derive the time-evolution equation for the equal-time density-current correlation $\mathcal{C}_r^{\eta Q}(t, t)$, which is presented in Eq. (35) of the main text. We write down all of the possible ways that the product $\eta_r Q_0$ can change in the infinitesimal time

interval $[t, t + dt]$, as given by

$$
\eta_r(t + dt)Q_0(t + dt) = \begin{cases}
1 \times (Q_0(t) + 1), & \text{prob.} \quad \mathcal{P}_r^3(t)dt \\
1 \times (Q_0(t) - 1), & \text{prob.} \quad \mathcal{P}_r^4(t)dt \\
0 \times (Q_0(t) + 1), & \text{prob.} \quad \mathcal{P}_r^5(t)dt \\
0 \times (Q_0(t) - 1), & \text{prob.} \quad \mathcal{P}_r^6(t)dt \\
\eta_r(t)(Q_0(t) + 1), & \text{prob.} \quad [\mathcal{P}_0^R(t) - \mathcal{P}_r^3(t) - \mathcal{P}_r^5(t)]dt \\
\eta_r(t)(Q_0(t) - 1), & \text{prob.} \quad [\mathcal{P}_0^L(t) - \mathcal{P}_r^4(t) - \mathcal{P}_r^6(t)]dt \\
1 \times Q_0(t), & \text{prob.} \quad [\mathcal{P}_r^+(t) - \mathcal{P}_r^3(t) - \mathcal{P}_r^4(t)]dt \\
0 \times Q_0(t), & \text{prob.} \quad [\mathcal{P}_r^-(t) - \mathcal{P}_r^5(t) - \mathcal{P}_r^6(t)]dt \\
\eta_r(t)Q_0(t), & \text{prob.} \quad 1 - \hat{\Sigma}(t)dt,
\end{cases}
\tag{C1}
$$

where $\hat{\Sigma}(t)dt$ is the sum of probability operators corresponding to all the possible ways in which the product $\eta_r(t)Q_0(t)$ can change in the infinitesimal time interval dt and is given by

$$
\hat{\Sigma}(t) = \mathcal{P}_r^+(t) + \mathcal{P}_r^-(t) + \mathcal{P}_0^R(t) + \mathcal{P}_0^L(t) + \mathcal{P}_r^3(t) + \mathcal{P}_r^4(t) + \mathcal{P}_r^5(t) + \mathcal{P}_r^6(t),
\tag{C2}
$$

and the operators $\mathcal{P}_r^3(t)$, $\mathcal{P}_r^4(t)$, $\mathcal{P}_r^5(t)$, and $\mathcal{P}_r^6(t)$ are defined as

$$
\mathcal{P}_r^3(t) = \frac{1}{2} \sum_{l=1}^{\infty} \phi(l) \left[\left(\mathcal{U}_r^{(l)} - \mathcal{U}_r^{(l+1)} \right) \sum_{k=1}^{l} \delta_{r,k} + \sum_{g=1}^{l-1} \mathcal{V}_{r+1}^{(g+2)} \sum_{k=1}^{g} \delta_{r,k} \right],
\tag{C3}
$$

$$
\mathcal{P}_r^4(t) = \frac{1}{2} \sum_{l=1}^{\infty} \phi(l) \left[\left(\mathcal{U}_{r+l-1}^{(l)} - \mathcal{U}_{r+l}^{(l+1)} \right) \sum_{k=1}^{l} \delta_{r,-k+1} + \sum_{g=1}^{l-1} \mathcal{V}_{r+g}^{(g+2)} \sum_{k=1}^{g} \delta_{r,-k+1} \right],
\tag{C4}
$$

$$
\mathcal{P}_r^5(t) = \frac{1}{2} \sum_{l=1}^{\infty} \phi(l) \left[\left(\mathcal{U}_{r+l}^{(l)} - \mathcal{U}_{r+l}^{(l+1)} \right) \sum_{k=1}^{l} \delta_{r,-k+1} + \sum_{g=1}^{l-1} \mathcal{V}_{r+g+1}^{(g+2)} \sum_{k=1}^{g} \delta_{r,-k+1} \right],
\tag{C5}
$$

$$
\mathcal{P}_r^6(t) = \frac{1}{2} \sum_{l=1}^{\infty} \phi(l) \left[\left(\mathcal{U}_{r-1}^{(l)} - \mathcal{U}_r^{(l+1)} \right) \sum_{k=1}^{l} \delta_{r,k} + \sum_{g=1}^{l-1} \mathcal{V}_r^{(g+2)} \sum_{k=1}^{g} \delta_{r,k} \right].
\tag{C6}
$$

Using the above update rules, shown in Eq. (C1), the time evolution of the quantity $\langle \eta_r(t)Q_0(t) \rangle$ is given by

$$
\frac{d}{dt} \langle \eta_r(t)Q_0(t) \rangle = \left[\langle \mathcal{P}_r^3(t) \rangle - \langle \mathcal{P}_r^4(t) \rangle - \langle \mathcal{P}_r^5(t) \rangle + \langle \mathcal{P}_r^6(t) \rangle \right] + \langle [\mathcal{P}_r^+(t) - \mathcal{P}_r^-(t)]Q_0(t) \rangle + \langle \eta_r(t)[\mathcal{P}_0^R(t) - \mathcal{P}_0^L(t)] \rangle.
\tag{C7}
$$

At the steady state, we can disregard the spatial dependence in the average quantities $\langle \mathcal{U}^{(l)} \rangle$ and $\langle \mathcal{V}^{(g+2)} \rangle$, which essentially leads to the simplification of the first term in Eq. (C7) in the following manner:

$$
\langle \mathcal{P}_r^3(t) \rangle - \langle \mathcal{P}_r^4(t) \rangle - \langle \mathcal{P}_r^5(t) \rangle + \langle \mathcal{P}_r^6(t) \rangle = \sum_{l=1}^{\infty} \phi(l) \left[(\mathcal{U}^{(l)} - \mathcal{U}^{(l+1)}) \sum_{k=1}^{l} (\delta_{r,k} - \delta_{r,-k+1}) + \sum_{g=1}^{l-1} \mathcal{V}^{(g+2)} \sum_{k=1}^{g} (\delta_{r,k} - \delta_{r,-k+1}) \right].
\tag{C8}
$$

Moreover, using the identity shown in Eq. (B7), the second term in Eq. (C7) can be transformed into

$$
\langle [\mathcal{P}_r^+(t) - \mathcal{P}_r^-(t)]Q_0(t) \rangle \simeq D(\rho, \gamma)\Delta_r^2 \langle \eta_r(t)Q_0(t) \rangle.
\tag{C9}
$$

Furthermore, using the following relation, $\mathcal{P}_0^R(t) - \mathcal{P}_0^L(t) = J_0^{(D)}(t) \simeq D(\rho, \gamma)(\eta_0 - \eta_1)$, we rewrite the third term in Eq. (C7) in the following way:

$$
\langle \eta_r(t)[\mathcal{P}_0^R(t) - \mathcal{P}_0^L(t)] \rangle \simeq D(\rho, \gamma)[\langle \eta_r(t)\eta_0(t) \rangle - \langle \eta_r(t)\eta_1(t) \rangle] = D(\rho, \gamma)\Delta_r \langle \eta_r(t)\eta_0(t) \rangle.
\tag{C10}
$$

Finally, using the last three transformations, the time-evolution equation of $\mathcal{C}_r^{\eta Q}(t, t)$ can be written as the following inhomogeneous differential equation:

$$
\frac{d}{dt} \mathcal{C}_r^{\eta Q}(t, t) \simeq D(\rho, \gamma)\Delta_r^2 \mathcal{C}_r^{\eta Q}(t, t) + \mathcal{S}_r^{\eta Q}(t),
\tag{C11}
$$

where the source term is given by

$$
\mathcal{S}_r^{\eta Q}(t) = \sum_{l=1}^{\infty} \phi(l) \left[(\mathcal{U}^{(l)} - \mathcal{U}^{(l+1)}) \sum_{k=1}^{l} (\delta_{r,k} - \delta_{r,-k+1}) + \sum_{g=1}^{l-1} \mathcal{V}^{(g+2)} \sum_{k=1}^{g} (\delta_{r,k} - \delta_{r,-k+1}) \right] + D(\rho, \gamma)\Delta_r \mathcal{C}_r^{\eta\eta}(t, t).
\tag{C12}
$$

Equation (C11) describes the time evolution of $\mathcal{C}_r^{\eta Q}(t, t)$ in the real space, which in the Fourier space is simply transformed into the following equation:

$$\left(\frac{d}{dt} + D(\rho, \gamma)\lambda_q\right)\tilde{\mathcal{C}}_q^{\eta Q}(t, t) = \tilde{\mathcal{S}}_q^{\eta Q}(t). \tag{C13}$$

Note that the above equation appears in Eq. (35) in the main text. Here $-\lambda_q$ is the eigenvalue of the discrete Laplacian operator, which is given by

$$\lambda_q = 2(1 - \cos(q)), \tag{C14}$$

and $\tilde{\mathcal{S}}_q^{\eta Q}(t)$ is the source term in the Fourier space which is trivially obtained to be

$$\tilde{\mathcal{S}}_q^{\eta Q}(t) = \frac{1}{(1 - e^{-iq})}\left[D(\rho, \gamma)\lambda_q\tilde{\mathcal{C}}_q^{\eta\eta}(t, t) - \sum_{l=1}^{\infty}\phi(l)\left\{(\mathcal{U}^{(l)} - \mathcal{U}^{(l+1)})\lambda_{lq} + \sum_{g=1}^{l-1}\mathcal{V}^{(g+2)}\lambda_{gq}\right\}\right]. \tag{C15}$$

Finally, using the following identities that relate the correlators $\mathcal{U}^{(l)}$, $\mathcal{V}^{(g+2)}$ with the gap-distribution function $P(g)$ as given by

$$\mathcal{U}^{(l)}(t) = \rho\sum_{g=l-1}^{\infty}(g - l + 1)P(g, t),$$

$$\mathcal{V}^{(g+2)}(t) = \rho P(g, t), \tag{C16}$$

we obtain simpler structure of $\tilde{\mathcal{S}}_q^{\eta Q}(t)$, which is given by

$$\tilde{\mathcal{S}}_q^{\eta Q}(t) = \frac{1}{(1 - e^{-iq})}\left[D(\rho, \gamma)\lambda_q\tilde{\mathcal{C}}_q^{\eta\eta}(t, t) - f_q(t)\right], \tag{C17}$$

where $f_q(t)$ is given by

$$f_q(t) = \rho\sum_{l=1}^{\infty}\phi(l)\left[\sum_{g=1}^{l-1}\lambda_{gq}P(g, t) + \lambda_{lq}\sum_{g=l}^{\infty}P(g, t)\right]. \tag{C18}$$

The last two equations compositely express the source term corresponding to the equal-time density-current correlation function and they appear in the main text in Eqs. (36) and (37), respectively.

APPENDIX D: TIME EVOLUTION OF EQUAL-TIME DENSITY-DENSITY CORRELATION $\mathcal{C}_r^{\eta\eta}(t, t)$

$$\eta_r(t + dt)\eta_0(t + dt) = \begin{cases} 1 \times 1, & \text{prob.} \quad \mathcal{P}_r^7(t)dt \\ 0 \times 0, & \text{prob.} \quad \mathcal{P}_r^8(t)dt \\ 1 \times 0, & \text{prob.} \quad \mathcal{P}_r^9(t)dt \\ 0 \times 1, & \text{prob.} \quad \mathcal{P}_r^{10}(t)dt \\ 1 \times \eta_0(t), & \text{prob.} \quad \left[\mathcal{P}_r^+(t) - \mathcal{P}_r^7(t) - \mathcal{P}_r^9(t)\right]dt \\ 0 \times \eta_0(t), & \text{prob.} \quad \left[\mathcal{P}_r^-(t) - \mathcal{P}_r^8(t) - \mathcal{P}_r^{10}(t)\right]dt \\ \eta_r(t) \times 1, & \text{prob.} \quad \left[\mathcal{P}_0^+(t) - \mathcal{P}_r^7(t) - \mathcal{P}_r^{10}(t)\right]dt \\ \eta_r(t) \times 0, & \text{prob.} \quad \left[\mathcal{P}_0^-(t) - \mathcal{P}_r^8(t) - \mathcal{P}_r^9(t)\right]dt \\ \eta_r(t)\eta_0(t), & \text{prob.} \quad 1 - \hat{\Sigma}(t)dt, \end{cases} \tag{D1}$$

where $\hat{\Sigma}(t)dt$ corresponds to the total probability with which the product of occupations at sites r and 0 changes in the infinitesimal time interval dt with

$$\hat{\Sigma}(t) = \mathcal{P}_r^+(t) + \mathcal{P}_r^-(t) + \mathcal{P}_0^+(t) + \mathcal{P}_0^-(t) - \mathcal{P}_r^7(t) - \mathcal{P}_r^8(t) - \mathcal{P}_r^9(t) - \mathcal{P}_r^{10}(t), \tag{D2}$$

and the operators $\mathcal{P}_r^7(t)$, $\mathcal{P}_r^8(t)$, $\mathcal{P}_r^9(t)$, and $\mathcal{P}_r^{10}(t)$ are defined as

$$\mathcal{P}_r^7(t) = \frac{1}{2}\sum_{l=1}^{\infty}\phi(l)\left[\sum_{g=1}^{l-1}\left(\mathcal{V}_{r+1}^{(g+2)} + \mathcal{V}_{r+g}^{(g+2)}\right)\delta_{r,0} + \left\{(\mathcal{U}_r^{(l)} - \mathcal{U}_r^{(l+1)}) + (\mathcal{U}_{r+l-1}^{(l)} - \mathcal{U}_{r+l}^{(l+1)})\right\}\delta_{r,0}\right], \tag{D3}$$

$$\mathcal{P}_r^8(t) = \frac{1}{2} \sum_{l=1}^{\infty} \phi(l) \left[\sum_{g=1}^{l-1} \left(\mathcal{V}_r^{(g+2)} + \mathcal{V}_{r+g+1}^{(g+2)} \right) \delta_{r,0} + \left\{ \left(\mathcal{U}_{r+l}^{(l)} - \mathcal{U}_{r+l}^{(l+1)} \right) + \left(\mathcal{U}_{r-1}^{(l)} - \mathcal{U}_r^{(l+1)} \right) \right\} \delta_{r,0} \right], \tag{D4}$$

$$\mathcal{P}_r^9(t) = \frac{1}{2} \sum_{l=1}^{\infty} \phi(l) \left[\sum_{g=1}^{l-1} \left(\mathcal{V}_{g+1}^{(g+2)} \delta_{r,g} + \mathcal{V}_0^{(g+2)} \delta_{r,-g} \right) + \left\{ \left(\mathcal{U}_l^{(l)} - \mathcal{U}_l^{(l+1)} \right) \delta_{r,l} + \left(\mathcal{U}_{-1}^{(l)} - \mathcal{U}_0^{(l+1)} \right) \delta_{r,-l} \right\} \right], \tag{D5}$$

$$\mathcal{P}_r^{10}(t) = \frac{1}{2} \sum_{l=1}^{\infty} \phi(l) \left[\sum_{g=1}^{l-1} \left(\mathcal{V}_{r+g+1}^{(g+2)} \delta_{r,-g} + \mathcal{V}_r^{(g+2)} \delta_{r,g} \right) + \left\{ \left(\mathcal{U}_{r+l}^{(l)} - \mathcal{U}_{r+l}^{(l+1)} \right) \delta_{r,-l} + \left(\mathcal{U}_{r-1}^{(l)} - \mathcal{U}_r^{(l+1)} \right) \delta_{r,l} \right\} \right]. \tag{D6}$$

Finally, using the above update rules in Eq. (D1), we can straightforwardly write down the corresponding time-evolution equation, which is given by

$$\frac{d}{dt} \langle \eta_r(t) \eta_0(t) \rangle = \left(\langle \mathcal{P}_r^7(t) \rangle + \langle \mathcal{P}_r^8(t) \rangle - \langle \mathcal{P}_r^9(t) \rangle - \langle \mathcal{P}_r^{10}(t) \rangle \right) + \langle \eta_r(t) (\mathcal{P}_0^+(t) - \mathcal{P}_0^-(t)) \rangle + \langle (\mathcal{P}_r^+(t) - \mathcal{P}_r^-(t)) \eta_0(t) \rangle. \tag{D7}$$

Using the concept of spatial homogeneity at the steady state, we can now ignore the spatial dependence in the averages $\langle \mathcal{U}^{(l)} \rangle$ and $\langle \mathcal{V}^{(g+2)} \rangle$, which leads to the following simplification of the first term in Eq. (D7):

$$\mathcal{S}_r^{\eta\eta}(t) = \langle \mathcal{P}_r^7(t) \rangle + \langle \mathcal{P}_r^8(t) \rangle - \langle \mathcal{P}_r^9(t) \rangle - \langle \mathcal{P}_r^{10}(t) \rangle$$

$$= \sum_{l=1}^{\infty} \phi(l) \left[\sum_{g=1}^{l-1} \mathcal{V}^{(g+2)}(t) \left(2\delta_{r,0} - \delta_{r,g} - \delta_{r,-g} \right) + (\mathcal{U}^{(l)}(t) - \mathcal{U}^{(l+1)}(t)) (2\delta_{r,0} - \delta_{r,l} - \delta_{r,-l}) \right]$$

$$= \rho \sum_{l=1}^{\infty} \phi(l) \left[\sum_{g=1}^{l-1} P(g,t) (2\delta_{r,0} - \delta_{r,g} - \delta_{r,-g}) + \sum_{g=l}^{\infty} P(g,t) (2\delta_{r,0} - \delta_{r,l} - \delta_{r,-l}) \right]. \tag{D8}$$

Note that in the last line we have used the identities in Eq. (C16) to replace the correlators $\mathcal{V}^{(g+2)}(t)$ and $\mathcal{U}^{(l)}(t)$ in terms of the gap-distribution function $P(g, t)$. Furthermore, using the second identity, shown in Eq. (B7), and the definition of $\mathcal{C}_r^{\eta\eta}(t, t)$, we can write down the corresponding time-evolution equation in real space in the following manner:

$$\frac{d}{dt} \mathcal{C}_r^{\eta\eta}(t, t) = 2D(\rho, \gamma) \Delta_r^2 \mathcal{C}_r^{\eta\eta}(t, t) + \mathcal{S}_r^{\eta\eta}(t). \tag{D9}$$

In fact, using Eq. (27) in the above equation, we immediately obtain the corresponding evolution equation in the Fourier space, which is given by

$$\frac{d}{dt} \tilde{\mathcal{C}}_q^{\eta\eta}(t, t) + 2D(\rho, \gamma) \lambda_q \tilde{\mathcal{C}}_q^{\eta\eta}(t, t) = \tilde{\mathcal{S}}_q^{\eta\eta}(t), \tag{D10}$$

where $\tilde{\mathcal{S}}_q^{\eta\eta}(t)$ is the corresponding source term in the Fourier space, which is simply obtained by using Eq. (27) in Eq. (D8) and is given by

$$\tilde{\mathcal{S}}_q^{\eta\eta}(t) = \rho \sum_{l=1}^{\infty} \phi(l) \left[\sum_{g=1}^{l-1} \lambda_{gq} P(g,t) + \lambda_{lq} \sum_{g=l}^{\infty} P(g,t) \right]. \tag{D11}$$

It is worth noting that Eq. (D10) is the desired equation used in the main text as Eq. (40).

APPENDIX E: TIME EVOLUTION OF EQUAL-TIME CURRENT-CURRENT CORRELATION $\mathcal{C}_r^{QQ}(t, t)$

Here we provide the derivation details of Eq. (45) in the main text, which describes the time evolution of $\mathcal{C}_r^{QQ}(t, t)$. We begin with the update rules corresponding to $Q_r(t) Q_0(t)$, as written below:

$$Q_r(t+dt) Q_0(t+dt) = \begin{cases} (Q_r(t) + 1)(Q_0(t) + 1), & \text{prob.} \quad \mathcal{P}_r^1(t) dt \\ (Q_r(t) + 1) Q_0(t), & \text{prob.} \quad \left[\mathcal{P}_r^R(t) - \mathcal{P}_r^1(t) \right] dt \\ Q_r(t)(Q_0(t) + 1), & \text{prob.} \quad \left[\mathcal{P}_0^R(t) - \mathcal{P}_r^1(t) \right] dt \\ (Q_r(t) - 1)(Q_0(t) - 1), & \text{prob.} \quad \mathcal{P}_r^2(t) dt \\ (Q_r(t) - 1) Q_0(t), & \text{prob.} \quad \left[\mathcal{P}_r^L(t) - \mathcal{P}_r^2 \right] dt \\ Q_r(t)(Q_0(t) - 1), & \text{prob.} \quad \left[\mathcal{P}_0^L(t) - \mathcal{P}_r^2(t) \right] dt \\ Q_r(t) Q_0(t), & \text{prob.} \quad 1 - \hat{\Sigma}(t) dt, \end{cases} \tag{E1}$$

where $\hat{\Sigma}(t)dt$ corresponds to the total probability with which the product of currents across bonds $(r, r+1)$ and $(0,1)$ changes in the infinitesimal time interval dt with

$$\hat{\Sigma} = \mathcal{P}_r^R(t) + \mathcal{P}_0^R(t)) + \mathcal{P}_r^L(t) + \mathcal{P}_0^L(t)) - \mathcal{P}_r^1(t) - \mathcal{P}_r^2(t), \tag{E2}$$

and the operators $\mathcal{P}_r^1$ and $\mathcal{P}_r^2$ are defined as

$$\mathcal{P}_r^1 = \frac{1}{2}\sum_{l=1}^{\infty}\phi(l)\left\{\sum_{k=1}^{l}\left(\mathcal{U}_{r+k}^{(l)} - \mathcal{U}_{r+k}^{(l+1)}\right)\Theta(k+r)\Theta(l-r-k+1) + \sum_{g=1}^{l-1}\sum_{k=1}^{g}\mathcal{V}_{r+k+1}^{(g+2)}\Theta(k+r)\Theta(g-r-k+1)\right\},$$

$$\mathcal{P}_r^2 = \frac{1}{2}\sum_{l=1}^{\infty}\phi(l)\left\{\sum_{k=1}^{l}\left(\mathcal{U}_{r+k-1}^{(l)} - \mathcal{U}_{r+k}^{(l+1)}\right)\Theta(k+r)\Theta(l-r-k+1) + \sum_{g=1}^{l-1}\sum_{k=1}^{g}\mathcal{V}_{r+k}^{(g+2)}\Theta(k+r)\Theta(g-r-k+1)\right\}. \tag{E3}$$

Here $\Theta(r)$ is the Heaviside theta function, which is defined as

$$\Theta(r) = \begin{cases} 1 & \text{for } r > 0 \\ 0 & \text{otherwise.} \end{cases} \tag{E4}$$

Using the update rules shown in Eq. (E1), we write the evolution of the two-point equal-time current-current correlation as

$$\frac{d}{dt}\langle Q_r(t)Q_0(t)\rangle = \left[\langle\mathcal{P}_r^1\rangle + \langle\mathcal{P}_r^2\rangle\right] + \langle J_r^{(D)}(t)Q_0(t)\rangle + \langle J_0^{(D)}(t)Q_r(t)\rangle. \tag{E5}$$

At the steady state, we can ignore the position dependence in the averages $\langle\mathcal{P}_r^1\rangle$ and $\langle\mathcal{P}_r^2\rangle$, which leads us to write the first term in a simplified manner through the following quantity:

$$\Gamma_r = \langle\mathcal{P}_r^1\rangle + \langle\mathcal{P}_r^2\rangle$$

$$= \sum_{l=|r|+1}^{\infty}\phi(l)\left\{(\mathcal{U}^{(l)} - \mathcal{U}^{(l+1)})(l-|r|) + \sum_{g=1}^{l-1}\mathcal{V}^{(g+2)}(g-|r|)\right\} \tag{E6}$$

$$= \rho\sum_{l=|r|+1}^{\infty}\phi(l)\left\{(l-|r|)\sum_{g=l}^{\infty}P(g) + \sum_{g=1}^{l-1}(g-|r|)P(g)\right\}, \tag{E7}$$

where to arrive the last equation, which is presented as Eq. (46) in the main text, we have used the identities shown in Eq. (C16). Finally, using the definition of $\mathcal{C}_r^{QQ}(t,t)$ and the closure approximation scheme, as shown in Eq. (23), we obtain the desired time-evolution equation,

$$\frac{d}{dt}\mathcal{C}_r^{QQ}(t,t) = \Gamma_r - D(\rho,\gamma)\Delta_r\mathcal{C}_r^{\eta Q}(t,t) - D(\rho,\gamma)\Delta_{-r}\mathcal{C}_{-r}^{\eta Q}(t,t). \tag{E8}$$

By using Fourier transform in Eq. (28) in the main text, we now invert the $\mathcal{C}_r^{\eta Q}(t,t)$ and $\mathcal{C}_{-r}^{\eta Q}(t,t)$ in Eq. (E8) in their Fourier basis, and, as a result, the corresponding steady-state time-evolution equation of $\mathcal{C}_r^{QQ}(t,t)$ takes the following form:

$$\frac{d}{dt}\mathcal{C}_r^{QQ}(t,t) = \Gamma_r + \frac{D(\rho,\gamma)}{L}\sum_q(2-\lambda_{qr})(1-e^{-iq})\tilde{\mathcal{C}}_q^{\eta Q}(t,t). \tag{E9}$$

Equation (E9) is the resulting time-evolution equation, which is presented in the main text as Eq. (45) after integration.

APPENDIX F: TEMPORAL CORRELATION OF THE INSTANTANEOUS BOND CURRENT

Our aim in this section is to derive the expression of the steady-state temporal correlation of the instantaneous current $\mathcal{C}_0^{JJ}(t)$ in the long-time regime, which is presented in the main text in Eq. (60). Note that, for any time $t > 0$, we have already derived $\mathcal{C}_0^{JJ}(t)$ to obey the following equation [Eq. (59) in the main text]:

$$\mathcal{C}_0^{JJ}(t,0) = -\frac{D(\rho,\gamma)}{2L}\sum_q f_q e^{-\lambda_q D(\rho,\gamma)t}, \tag{F1}$$

where $q = 2\pi n/L$ with $n = 1, 2, \ldots, L-1$ and the quantity f_q at the steady state is defined as

$$f_q = \rho\sum_{l=1}^{\infty}\phi(l)\left[\sum_{g=1}^{l-1}\lambda_{gq}P(g) + \lambda_{lq}\sum_{g=l}^{\infty}P(g)\right], \tag{F2}$$

where $P(g)$ is the steady-state gap-distribution function of the system. Now, if we first take the infinite-system-size limit, i.e., $L \to \infty$, we have the following transformations: $q \to q(x) = 2\pi x$, $\lambda_q \to \lambda(x)$, and $f_q \to f(x)$. As a result, we can convert the summation into an integration, as shown in the following:

$$\lim_{L\to\infty}\mathcal{C}_0^{JJ}(t) \simeq -D(\rho,\gamma)\int_0^{1/2}dx f(x)e^{-\lambda(x)D(\rho,\gamma)t}. \tag{F3}$$

Interestingly, if we now take the large-time limit, i.e., $L^2/D \gg t \gg 1/D$ for $x > 0$, the integrand in Eq. (F3) contributes only in the limit $x \to 0$, while it becomes vanishingly small for any other x values. This effectively leads to performing a small-x analysis of Eq. (F3). Note that, in this limit of $x \to 0$, $\lambda(x)$ is quadratic, i.e., $\lambda(x) \to 4\pi^2 x^2$, $\lambda(lx) \to 4\pi^2 l^2 x^2$, and $\lambda(gx) \to 4\pi^2 g^2 x^2$. These transformations straightforwardly yield $f(x) \to 8\pi^2 x^2 \chi$, where χ is defined in Eq. (48) in the main text. Following all of the aforementioned transformations, Eq. (F3) in terms of a new variable $z = 4\pi^2 x^2 Dt$ is directly reduced to the following in the limit of large t:

$$\lim_{L \to \infty} \mathcal{C}_0^{JJ}(t) \simeq -\frac{\chi(\rho, \gamma)}{2\pi \sqrt{D(\rho, \gamma)}} t^{-3/2} \int_0^\infty dz \sqrt{z} e^{-z}. \quad (F4)$$

Finally, using $\int_0^\infty dz \sqrt{z} e^{-z} = \sqrt{\pi}/2$, we get the desired result presented in the main text in Eq. (60),

$$\mathcal{C}_0^{JJ}(t) \simeq -\frac{\chi(\rho, \gamma)}{4\sqrt{\pi D(\rho, \gamma)}} t^{-3/2}. \quad (F5)$$

APPENDIX G: DERIVATION OF THE TIME-INTEGRATED BOND-CURRENT FLUCTUATION $\mathcal{C}_0^{QQ}(t, t)$

According to Eq. (80) in the main text, the steady-state bond-current fluctuation for LLG is given by

$$\mathcal{C}_0^{QQ}(t, t) = \left[\Gamma_0 - \frac{1}{L} \sum_q \left(\frac{f_q}{\lambda_q} \right) \right] t$$
$$+ \frac{1}{LD} \sum_q \left(\frac{f_q}{\lambda_q^2} \right) (1 - e^{-\lambda_q Dt}), \quad (G1)$$

where we have defined f_q and λ_q in the main text in Eqs. (37) and (32), respectively. Moreover, in order to obtain Γ_0, we put $r = 0$ in Eq. (46) in the main text, and get

$$\Gamma_0 = \rho \sum_{l=1}^\infty \phi(l) \left\{ l \sum_{g=l}^\infty P(g) + \sum_{g=1}^{l-1} g P(g) \right\}. \quad (G2)$$

In order to simplify Eq. (G1), we first expand f_q and write

$$\sum_q \left(\frac{f_q}{\lambda_q} \right) = \rho \sum_{l=1}^\infty \phi(l) \left[\sum_{g=1}^{l-1} P(g) \sum_q \left(\frac{\lambda_{gq}}{\lambda_q} \right) \right.$$
$$\left. + \left(\sum_q \frac{\lambda_{lq}}{\lambda_q} \right) \sum_{g=l}^\infty P(g) \right]. \quad (G3)$$

Note that the wave vector is given by $q = 2\pi n/L$ where $n = 1, 2, 3, \ldots, L-1$. Therefore, the above summation over q, appearing at the right-hand side of the above equation, can be equivalently transformed over the integer variable n, which can be solved easily using *Mathematica* to have the following simplified form:

$$\sum_q \left(\frac{\lambda_{gq}}{\lambda_q} \right) = \sum_{n=1}^{L-1} \left(\frac{1 - \cos\left(\frac{2\pi gn}{L}\right)}{1 - \cos\left(\frac{2\pi n}{L}\right)} \right) = g(L - g), \quad (G4)$$

$$\sum_q \left(\frac{\lambda_{lq}}{\lambda_q} \right) = \sum_{n=1}^{L-1} \left(\frac{1 - \cos\left(\frac{2\pi ln}{L}\right)}{1 - \cos\left(\frac{2\pi n}{L}\right)} \right) = l(L - l). \quad (G5)$$

Applying these relations in Eq. (G3) drastically simplifies it and the resulting equation is given by

$$\sum_q \left(\frac{f_q}{\lambda_q} \right) = L\Gamma_0 - 2\chi(\rho, \gamma). \quad (G6)$$

Using the above equation in Eq. (G1), we finally obtain the expression of $\mathcal{C}_0^{QQ}(t, t)$ used in the main text in Eq. (81), which is given by

$$\mathcal{C}_0^{QQ}(t, t) = \frac{2\chi(\rho, \gamma)}{L} t + \frac{1}{D(\rho, \gamma)L}$$
$$\times \sum_q \frac{f_q}{\lambda_q^2} \left(1 - e^{-\lambda_q D(\rho, \gamma)t}\right). \quad (G7)$$

APPENDIX H: LIMITING CASES OF $\mathcal{C}_0^{QQ}(t, t)$

In this section, we are going to calculate $\mathcal{C}_0^{QQ}(t, t)$ in three distinct time regimes, which is shown in Eq. (84) in the main text.

1. Case I: $t \ll 1/D$

It is easy to check that, in this particular time regime, the second and third terms in Eq. (G1) identically cancel each other, which ultimately results in the following:

$$\mathcal{C}_0^{QQ}(t, t) = \Gamma_0 t. \quad (H1)$$

2. Case II: $1/D \ll t \ll L^2/D$

In order to calculate $\mathcal{C}_0^{QQ}(t, t)$ in the intermediate regime, we use the expression derived in Eq. (H2) and follow the footsteps of the analysis in Appendix F. As before, for infinitely large system size, i.e., $L \to \infty$, one can convert the summation into the following integral form:

$$\mathcal{C}_0^{QQ}(t, t) = \frac{2\chi(\rho, \gamma)}{L} t$$
$$+ \frac{2}{D(\rho, \gamma)} \int_0^{1/2} \frac{f(x) dx}{\lambda^2(x)} (1 - e^{-\lambda(x)D(\rho, \gamma)t}), \quad (H2)$$

where we have used the transformations $q = 2\pi n/L \equiv 2\pi x$, $\lambda_q \to \lambda(x)$, and $f_q \to f(x)$. Note that the integrand in the above equation primarily contributes to the limit $x \to 0$, in which case, following Eqs. (32) and (37) in the main text, we can write $\lambda(x) \simeq 4\pi^2 x^2$ and $f(x) \simeq 8\pi^2 x^2 \chi$. Finally, using the aforementioned transformations, the above equation in terms of a new variable, $z = 4\pi^2 x^2 Dt$, can be written as

$$\mathcal{C}_0^{QQ}(t, t) = \frac{2\chi(\rho, \gamma)}{L} t + \frac{\chi(\rho, \gamma)}{\pi \sqrt{D(\rho, \gamma)}} \int_0^\infty z^{-3/2} (1 - e^{-z}) dz. \quad (H3)$$

Finally, using the relation $\int_0^\infty z^{-3/2}(1 - e^{-z}) dz = 2\sqrt{\pi}$ and neglecting the first term which is a subleading contributor, the leading-order contribution to $\mathcal{C}_0^{QQ}(t, t)$ can be written as

$$\mathcal{C}_0^{QQ}(t, t) \simeq \frac{2\chi(\rho, \gamma)}{\sqrt{\pi D(\rho, \gamma)}} \sqrt{t} + \mathcal{O}(t), \quad (H4)$$

which is presented in the main text in Eq. (84).

3. Case III: $L^2/D \ll t$

From Eq. (H2), it is straightforward to see that, in the limit of large t such that $t \gg L^2/D$, the exponential term contributes nothing, whereas the second term gives a constant value and the leading-order contribution comes directly from the first term, which shows linear growth of $\mathcal{C}_0^{QQ}(t, t)$ with t, and the resulting equation becomes

$$\mathcal{C}_0^{QQ}(t, t) = \frac{2\chi(\rho, \gamma)}{L} t. \tag{H5}$$

APPENDIX I: SCALING RELATION OF THE EFFECTIVE MOBILITY $\chi(\rho, \gamma)$

In this section, we will obtain the scaling relation for $\chi(\rho, \gamma)$ in the limit $\rho \to 0$, $\gamma \to 0$, such that the ratio $\psi = \rho/\gamma$ is finite, and calculate the corresponding scaling function $\mathcal{H}(\psi)$ shown in the main text in Eqs. (77) and (79). We begin our analysis with the expression $\chi(\rho, \gamma)$ shown in Eq. (48) in the main text, i.e.,

$$\chi(\rho, \gamma) = \frac{\rho}{2} \sum_{l=1}^{\infty} \phi(l) \left[\sum_{g=1}^{l-1} g^2 P(g) + l^2 \sum_{g=l}^{\infty} P(g) \right]. \tag{I1}$$

Note that the hop-length distribution $\phi(l)$ is given in Eq. (2) in the main text as

$$\phi(l) = A e^{-\gamma l}, \tag{I2}$$

where the normalization constant $A = (1 - e^{-1/l_p})$. Moreover, the steady-state gap-distribution function $P(g)$, which is assumed to be exponentially distributed for $g > 0$, has the following form:

$$P(g) \simeq N_* \exp(-g/g_*), \tag{I3}$$

where the prefactor N_*, as shown in the main text in Eq. (54), is given by

$$N_* = \left(\frac{1}{\rho} - 1 \right) \frac{(e^{1/g_*} - 1)^2}{e^{1/g_*}}. \tag{I4}$$

Now, using the above expression of $P(g)$ in Eq. (I1) and performing some algebraic manipulations, we obtain

$$\chi(\rho, \gamma) = \frac{(1 - \rho)}{2} \frac{(e^{1/g_*} - 1)(e^{\gamma + 1/g_*} + 1)}{(e^{\gamma + 1/g_*} - 1)^2}. \tag{I5}$$

Note that the above expression of $\chi(\rho, \gamma)$ is valid for any arbitrary ρ and γ. However, in the following analysis, we look at two specific cases: *Case I*, $\rho \to 0$ *and* $\gamma \to \infty$. In this case, the typical gap size g_* is given by

$$g_* = \frac{1}{\rho}. \tag{I6}$$

Now, to calculate $\chi(\rho, \gamma)$, we use Eq. (I6) in Eq. (I5), and with the limit $\rho \to 0$ such that $\gamma + 1/g_* \simeq \gamma \gg 1$ in consideration, we obtain

$$\chi(\rho, \gamma) = \frac{(e^\rho - 1)(1 - \rho)}{2} e^{-\gamma} \tag{I7}$$

$$\simeq \frac{\rho(1 - \rho)}{2} e^{-\gamma} = \frac{\chi^{(0)} e^{-\gamma}}{2}, \tag{I8}$$

where $\chi^{(0)} = \rho(1 - \rho)$ is the particle mobility in SSEP.

Case II, $\rho \to 0$ *and* $\gamma \to 0$. In the limit of $\rho \to 0$, $\gamma \to 0$, such that the ratio $\psi = \rho/\gamma$ is finite, we make the following transformations in Eq. (I5):

(a) The typical gap size g_* obeys the following scaling relation:

$$g_* \simeq \frac{1}{\rho} \mathcal{G}(\psi), \tag{I9}$$

where $\mathcal{G}(\psi)$ is the scaling function corresponding to g_*, which upon consideration of the two limiting cases is assumed to be $\mathcal{G}(\psi) = \sqrt{1 + \psi}$ [see the paragraph before Eq. (77) in the main text].

(b) All the exponential terms are approximated up to the leading-order contributions, i.e.,

$$e^{\gamma + 1/g_*} - 1 \simeq \gamma + 1/g_* = \gamma + \rho/\mathcal{G}(\psi) = \gamma(1 + \psi/\mathcal{G}(\psi)), \tag{I10}$$

$$e^{1/g_*} - 1 \simeq 1/g_* = \gamma\psi/\mathcal{G}(\psi), \tag{I11}$$

$$e^{\gamma + 1/g_*} + 1 \simeq 2. \tag{I12}$$

Finally, by substituting the above transformation in Eq. (I5), we get the leading-order contribution to $\chi(\rho, \gamma)$ in the limit $\rho \to 0$ and $\gamma \to 0$, as shown below:

$$\chi(\rho, \gamma) \simeq \frac{\rho(1 - \rho)}{\gamma^2} \frac{\mathcal{G}(\psi)}{(\psi + \mathcal{G}(\psi))^2}. \tag{I13}$$

Note that, by replacing $\chi^{(0)} = \rho(1 - \rho)$ in the above equation, we immediately obtain the scaling relation shown in Eq. (77) in the main text and the corresponding scaling function is given by

$$\mathcal{H}(\psi) = \frac{\mathcal{G}(\psi)}{(\psi + \mathcal{G}(\psi))^2}. \tag{I14}$$

[1] M. C. Marchetti, J. F. Joanny, S. Ramaswamy, T. B. Liverpool, J. Prost, M. Rao, and R. A. Simha, Rev. Mod. Phys. **85**, 1143 (2013).

[2] C. Bechinger, R. Di Leonardo, H. Löwen, C. Reichhardt, G. Volpe, and G. Volpe, Rev. Mod. Phys. **88**, 045006 (2016).

[3] T. Vicsek, A. Czirók, E. Ben-Jacob, I. Cohen, and O. Shochet, Phys. Rev. Lett. **75**, 1226 (1995).

[4] M. E. Cates and J. Tailleur, Annu. Rev. Condens. Matter Phys. **6**, 219 (2015).

[5] V. Narayan, S. Ramaswamy, and N. Menon, Science **317**, 105 (2007).

[6] S. C. Takatori, R. De Dier, J. Vermant, and J. F. Brady, Nat. Commun. **7**, 10694 (2016).

[7] P. Dolai, A. Das, A. Kundu, C. Dasgupta, A. Dhar, and K. V. Kumar, Soft Matter **16**, 7077 (2020).

[8] Y. Fily and M. C. Marchetti, Phys. Rev. Lett. **108**, 235702 (2012).

[9] J. Tailleur and M. E. Cates, Phys. Rev. Lett. **100**, 218103 (2008).

[10] L. Bertini, A. De Sole, D. Gabrielli, G. Jona-Lasinio, and C. Landim, Rev. Mod. Phys. **87**, 593 (2015).

[11] S. Katz, J. L. Lebowitz, and H. Spohn, J. Stat. Phys. **34**, 497 (1984).

[12] S. Hanna, W. Hess, and R. Klein, J. Phys. A: Math. Gen. **14**, L493 (1981).

[13] A. De Masi and P. A. Ferrari, J. Stat. Phys. **107**, 677 (2002).

[14] T. Chakraborty and P. Pradhan, companion paper, Phys. Rev. E **109**, 024124 (2024).

[15] C. Arita, P. L. Krapivsky, and K. Mallick, Phys. Rev. E **90**, 052108 (2014).

[16] A. Mukherjee and P. Pradhan, Phys. Rev. E **107**, 024109 (2023).

[17] J. Bialké, H. Löwen, and T. Speck, Europhys. Lett. **103**, 30008 (2013).

[18] S. D. Cengio, D. Levis, and I. Pagonabarraga, Phys. Rev. Lett. **123**, 238003 (2019).

[19] T. Bodineau and B. Derrida, Phys. Rev. Lett. **92**, 180601 (2004).

[20] N. Katyal, S. Dey, D. Das, and S. Puri, Eur. Phys. J. E **43**, 10 (2020).

[21] L. Caprini, U. M. B. Marconi, and A. Puglisi, Phys. Rev. Lett. **124**, 078001 (2020).

[22] L. Caprini, U. M. B. Marconi, C. Maggi, M. Paoluzzi, and A. Puglisi, Phys. Rev. Res. **2**, 023321 (2020).

[23] L. Caprini and U. M. B. Marconi, Soft Matter **17**, 4109 (2021).

[24] G. Szamel and E. Flenner, Europhys. Lett. **133**, 60002 (2021).

[25] S. Garcia, E. Hannezo, J. Elgeti, J.-F. Joanny, P. Silberzan, and N. S. Gov, Proc. Natl. Acad. Sci. USA **112**, 15314 (2015).

[26] A. Cavagna, D. Conti, C. Creato, L. Del Castello, I. Giardina, T. S. Grigera, S. Melillo, L. Parisi, and M. Viale, Nat. Phys. **13**, 914 (2017).

[27] S. Henkes, K. Kostanjevec, J. M. Collinson, R. Sknepnek, and E. Bertin, Nat. Commun. **11**, 1405 (2020).

[28] Y.-E. Keta, R. L. Jack, and L. Berthier, Phys. Rev. Lett. **129**, 048002 (2022).

[29] B. Derrida and J. L. Lebowitz, Phys. Rev. Lett. **80**, 209 (1998).

[30] R. Harris, A. Rákos, and G. M. Schütz, J. Stat. Mech.: Theory Exp. (2005) P08003.

[31] C. Appert-Rolland, B. Derrida, V. Lecomte, and F. van Wijland, Phys. Rev. E **78**, 021122 (2008).

[32] B. Derrida and A. Gerschenfeld, J. Stat. Phys. **136**, 1 (2009).

[33] T. Sadhu and B. Derrida, J. Stat. Mech.: Theory Exp. (2016) 113202.

[34] L. Bertini, A. De Sole, D. Gabrielli, G. Jona-Lasinio, and C. Landim, Phys. Rev. Lett. **94**, 030601 (2005).

[35] B. Derrida and A. Gerschenfeld, J. Stat. Phys. **137**, 978 (2009).

[36] F. Cagnetta, F. Corberi, G. Gonnella, and A. Suma, Phys. Rev. Lett. **119**, 158002 (2017).

[37] T. Banerjee, R. L. Jack, and M. E. Cates, J. Stat. Mech.: Theory Exp. (2022) 013209.

[38] T. Bertrand, Y. Zhao, O. Bénichou, J. Tailleur, and R. Voituriez, Phys. Rev. Lett. **120**, 198103 (2018).

[39] P. Rizkallah, A. Sarracino, O. Bénichou, and P. Illien, Phys. Rev. Lett. **128**, 038001 (2022).

[40] T. Banerjee, S. N. Majumdar, A. Rosso, and G. Schehr, Phys. Rev. E **101**, 052101 (2020).

[41] T. GrandPre and D. T. Limmer, Phys. Rev. E **98**, 060601(R) (2018).

[42] M. Kourbane-Houssene, C. Erignoux, T. Bodineau, and J. Tailleur, Phys. Rev. Lett. **120**, 268003 (2018).

[43] T. Agranov, S. Ro, Y. Kafri, and V. Lecomte, J. Stat. Mech.: Theory Exp. (2021) 083208.

[44] T. Agranov, S. Ro, Y. Kafri, and V. Lecomte, SciPost Phys. **14**, 045 (2023).

[45] S. Jose, R. Dandekar, and K. Ramola, J Stat. Mech. (2023) 083208.

[46] A. B. Slowman, M. R. Evans, and R. A. Blythe, Phys. Rev. Lett. **116**, 218101 (2016).

[47] R. Soto and R. Golestanian, Phys. Rev. E **89**, 012706 (2014).

[48] T. Chakraborty, S. Chakraborti, A. Das, and P. Pradhan, Phys. Rev. E **101**, 052611 (2020).

[49] S. Chakraborti, T. Chakraborty, A. Das, R. Dandekar, and P. Pradhan, Phys. Rev. E **103**, 042133 (2021).

[50] O. Granek, Y. Kafri, and J. Tailleur, Phys. Rev. Lett. **129**, 038001 (2022).

[51] A. Hazra, A. Mukherjee, and P. Pradhan, arXiv:2309.14705.

[52] R. Mandal, P. J. Bhuyan, P. Chaudhuri, C. Dasgupta, and M. Rao, Nat. Commun. **11**, 2581 (2020).